IEEE Access
Multidisciplinary | Rapid Review | Open Access Journal

Received 7 June 2023, accepted 3 July 2023, date of publication 10 July 2023, date of current version 13 July 2023.

Digital Object Identifier 10.1109/ACCESS.2023.3293739

TOPICAL REVIEW

An Overview of Recent Development of the Gap-Waveguide Technology for mmWave and Sub-THz Applications

WAI YAN YONG[1,2], (Member, IEEE), ABBAS VOSOOGH[3], ALIREZA BAGHERI[1,3], COEN VAN DE VEN[1,3], (Graduate Student Member, IEEE), ABOLFAZL HADADDI[3], AND ANDRÉS ALAYÓN GLAZUNOV[4], (Senior Member, IEEE)

[1]Department of Electrical Engineering, University of Twente, 7500 AE Enschede, The Netherlands
[2]Rohde & Schwarz GmbH & Company KG., 81671 Munich, Germany
[3]Gapwaves AB, 412 63 Gothenburg, Sweden
[4]Department of Science and Technology, Linköping University, 602 21 Norrköping, Sweden

Corresponding author: Wai Yan Yong (w.y.yongwaiyan@utwente.nl)

This work was supported by the European Union's Horizon 2020 Research and Innovation Program under the Marie Sklodowska-Curie Grant under Grant 766231—WAVECOMBE—H2020-MSCA-ITN-2017.

ABSTRACT The millimeter-wave (mmWave) and sub-terahertz (sub-THz) bands have received much attention in recent years for wireless communication and high-resolution imaging radar applications. The objective of this paper is to provide an overview of recent developments in the design and technical implementation of GW-based antenna systems and components. This paper begins by comparing the GW-transmission line to other widely used transmission lines for the mmWave and sub-THz bands. Furthermore, the basic operating principle and possible implementation technique of the GW-technology are briefly discussed. In addition, various antennas and passive components have been developed based on the GW-technology. Despite its advantages in controlling electromagnetic wave propagation, it is also widely used for the packaging of electronic components such as transceivers and power amplifiers. This article also provided an overview of the current manufacturing technologies that are commonly used for the fabrication of GW-components. Finally, the practical applications and industry interest in GW technology developments for mmWave and sub-THz applications have been scrutinized.

INDEX TERMS Antenna, artificial magnetic conductor (AMC), beamforming, filter, gap waveguide, manufacturing, metamaterial, millimeter-wave, packaging, terahertz (THz), waveguide.

I. INTRODUCTION

The emergence of new wireless applications such as autonomous vehicles, virtual and augmented reality, the Internet of Things (IoT), machine-to-machine (M2M) communication, and mobile services resembling broadband perspectives, requires a substantial upgrade of wireless communications systems. As a result, the demand for increased data traffic, user data throughput, and lowering delays in mobile cellular networks is increasing exponentially. Technologies operating at the millimeter-wave (mmWave) and sub-THz frequency bands have been identified as enablers to meet these increasing demands. However, to benefit from the attractively large bandwidth chunks available in this region of the electromagnetic spectrum, several challenges must be surmounted. Aside from dealing with the challenges associated with over-the-air propagation (such as free-space propagation loss, atmospheric absorption, scattering, and so on), which are being widely investigated by wireless communication engineers [1], [2], there is a need to devise radio frequency front-end (RFFE) systems that perform well at these frequency bands by the microwave and antenna engineers. In addition, the successful commercialization of mmWave and sub-THz systems depends on the availability

The associate editor coordinating the review of this manuscript and approving it for publication was Davide Ramaccia.

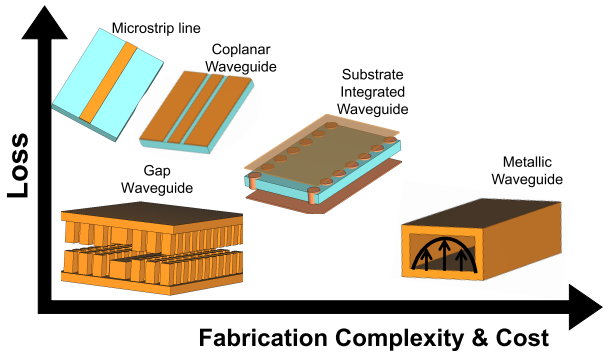

FIGURE 1. Comparison of the various transmission lines for mmWave and sub-THz bands in terms of loss versus fabrication complexity and cost.

of mass-production-ready and cost-effective technology. Furthermore, to minimize transmission losses, it has been predicted that high-density integration methods, particularly with conventional radio frequency (RF) components associated with a low-cost manufacturing process, should be available to provide a broad range of solutions for commercial products. Transmission line and packaging technologies are the foundation for making this vision a reality. Fig. 1 illustrates some commonly employed transmission lines for mmWave and sub-THz applications. One of the transmission line technologies that has attracted the most attention in the last decade is the so-called gap waveguide (GW) transmission line. In this paper, we intend to present as concisely as possible while covering the most relevant results of GW technology.

Let's start with an overview of existing transmission lines, which will provide a rationale for developing the gap waveguide (GW) technology. Planar transmission lines, such as microstrip lines and coplanar waveguides (CPWs), are compact and low-cost solutions based on printed circuit technologies. Since the 1950s, this type of transmission line has received extensive attention in developing passive circuits and antennas operating at the lower frequencies of the microwave spectrum. This technology offers straightforward structural integration, a low profile, lightweight, and topological miniaturization with mass-producibility at a low manufacturing cost [3]. Theoretically, any device, circuit, or antenna that operates at lower frequencies may be scaled up to operate at higher frequencies. There are no exclusions for mmWave and sub-THz approaches that might be created employing current low-frequency design platforms. However, shorter wavelengths at mmWave and sub-THz may increase design complexity and structural implementation. Indeed, transmission losses of these types of transmission lines become considerably high at these frequencies due to the higher dielectric losses, ohmic losses (as a result of the surface roughness and high-resistance of the narrow 50Ω microstrip line), and radiation leakage (due to surface-waves). Thus, realizing low-loss mmWave and sub-THz components such as filters and array antennas with microstrip lines is challenging. Although utilizing low-loss substrate technology such as Low-Temperature Co-Fired Ceramic (LTCC) [4] can deal with excessive dielectric losses in PCB, the conductor and radiation losses are inevitable. On the other hand, single-unit packaged components may improve the efficiency of the mmWave and sub-THz subsystems, but the radiation losses from these PCB strip lines can introduce other issues such as crosstalk, power, and signal integrity problems [5]. Despite its shortcomings, most mmWave and sub-THz monolithic microwave integrated circuits (MMIC) and RF modules are still manufactured and packaged employing this microstrip line technology; it remains a good candidate for designing a transition from the MMIC and RF module into other lower loss transmission lines [3].

The conventional hollow waveguide, on the other hand, is a more promising transmission line for mmWave and sub-THz communications in terms of loss-performance and power-handling capabilities [3], [5], [6]. The hollow waveguide is often entirely metallic, hence, providing a fully shielded waveguide transmission that avoids undesired radiation and dielectric losses since no dielectric substrate is needed. However, the non-planar features of the hollow waveguide make integration with other transmission lines challenging due to the complex transition design and the packaging issue. Furthermore, this waveguide structure is susceptible to manufacturing and assembly tolerances, particularly for multi-layer structures like array antenna designs, as good electrical contact is required between adjacent waveguide layers. Hollow waveguides are typically manufactured by first etching multi-layer metallic structures and then combining them employing a technique known as diffusion bonding [6]. The diffusion bonding process aims at providing stable surface bonding of the stack of metallic layers by employing plastic deformation and atom diffusion motion in a protective environment or vacuum under high pressure and high temperature ($\approx 1000°C$) conditions [6]. This type of bonding is necessary to ensure galvanic contact between the metallic layers of the stack, which is crucial to maintain the proper operation of the hollow waveguide. Although, with today's advanced technology, the manufacturing of the hollow waveguide has been substantially improved, this complicated manufacturing process is still expensive. Therefore, hollow waveguides remain unattractive for mass commercialization.

As an alternative technique, the substrate-integrated waveguide (SIW) or post-wall waveguide technology offers the combined benefits of both planar transmission lines and hollow waveguides [3], [5]. SIW structures are identical to rectangular dielectric-filled waveguide structures, except that two rows of metalized through holes replace the waveguide's short walls. Like the metal waveguide, the top and lower metal plates and through holes create a cross-sectional current loop. To minimize leakage, all of these through holes are put closely together [7]. Because of the vias on the sides, the transverse magnetic (TM) modes do not exist. Hence, this transmission line can only propagate TE_{m0} modes of

the conventional rectangular waveguide [5], [7]. However, because of the existence of the substrate, dielectric loss is unavoidable. For example, a SIW filter design at X-band might result in an insertion loss of roughly 2 dB [8], and as the frequency scales up to the W-band, the insertion loss can exceed 3 dB [9]. Furthermore, if the vias posts for the SIW are not properly designed and fabricated, undesirable leakage may occur, resulting in a degradation of the device's performance [5].

The performance gap of the above-explained transmission line technologies led to a quest for engineering new types of transmission lines offering low-loss performance and cost-effective manufacturing. In 2008, the late Professor Per-Simon Kildal invented the gap waveguide (GW) technology as a good candidate that fits the requirements of mmWave and sub-THz applications [10]. The GW technology builds upon prior research on hard and soft surfaces provided in [11]. The GW technology may be seen as a novel metamaterial-based wave-guiding structure that uses hard and soft boundary conditions to control electromagnetic wave propagation. The GW technology has recently been identified as one of the most promising transmission line technologies for mmWave and sub-THz communication because it combines the integration benefits of substrate-based technology with the low loss performance and high-power handling capability of conventional waveguides [12]. Furthermore, one of the most intriguing aspects of the GW technology is that it allows for an air gap between two layers without the need for an electrical connection, making the fabrication process considerably simpler and, therefore, far less expensive than diffusion bonding [10], [12]. Furthermore, the air gap has remedied the passive intermodulation issue that was frequently occurring due to the improper electrical contact between the waveguide-to-waveguide connection [13], [14], [15].

In this article, we present an overview of recent advancements in GW technology for mmWave and sub-THz antennas and circuits. The remaining organization of the paper is as follows. First, the fundamental notion of the GW is described, including various options to realize an artificial magnetic conductor and the corresponding GW-technology varieties. Second, several forms of GW-based antennas are examined and described, including array and phased array antennas, microstrip antennas, leaky-wave antennas, and horn antennas. Third, various passive circuits based on GW technology are presented, including beamforming networks, filters, and diplexers. This article also discusses and reports on the application of GW technology for packaging and integration with other transmission lines. Following that, the fabrication process that is typically utilized for the manufacturing of GW devices is outlined. Furthermore, practical applications and industrial interests are presented, together with essential references to patents being filed by the industry, demonstrating more and more the advancement of GW-based end-user devices and products. Lastly, the conclusion and recommendations for the future of GW technology research are provided.

II. FUNDAMENTALS OF GAP WAVEGUIDES

The fundamental operating principle of GW technology is guiding the propagation of electromagnetic waves via a parallel-plate waveguide [10]. In a conventional parallel-plate waveguide, which consists of two unconnected perfect electric conductors (PECs) parallel plates, Maxwell's equations solution for the propagation of electromagnetic waves exists, and thus, the propagation over the space separating them is possible. However, if one of these PEC plates is substituted with perfect magnetic conductors (PMCs) at a distance less than $\lambda/4$, no electromagnetic waves can propagate between them [10]. This is because when the air gap is smaller than $\lambda/4$, there is a cutoff of all propagating modes over the air gap that the PMC creates due to its high surface impedance characteristics. This feature, therefore, can be used to control the direction of propagation of the wave without leaking away into other directions. Therefore, if a section of this PMC region is replaced by a PEC (realized as a ridge, groove, or strip), then the electromagnetic waves will be forced to travel along this PEC channel [10]. Fig. 2 depicts the principle mentioned above. While existing metallic materials can approximately realize ideal PECs, PMCs do not exist naturally. However, it may be artificially engineered as an artificial magnetic conductor (AMC) or a high impedance surface [16].

As compared to the conventional transmission lines such as the microstrip and the hollow waveguide, the GW transmission line is an excellent contender for mmWave and THz applications because of its appealing properties, which include low loss, flexible planar manufacturing, and cost-effectiveness [10], [12]. The GW technology has a low loss performance, particularly for fully metallic-based GWs, since electromagnetic waves propagate unimpeded through the air along the permissible paths. The non-permissible paths impede wave propagation confining the wave propagation throughout the permissible region. Hence, a small air gap is tolerated between PEC-PMC plates [10]. This feature provides more manufacturing and assembly freedom by resolving the good electrical connection issues that emerge with conventional hollow waveguides. This leads to significant cost-savings in manufacturing.

Four different types of the GW-technology can be realized on the foundation of the principles presented above, which are outlined next.

A. REALIZATION OF THE AMC PINS FOR GAP WAVEGUIDE

As explained above, the AMC structures are essential to the design of the GW structures. These AMC structures provide a bandstop behavior over the operating frequencies of interests. This subsection discusses the various approaches for realizing the AMC structures for the practical realization of GWs. These AMC structures may be realized by employing mushroom-like pins or glide-symmetry holey structures as illustrated in Fig. 3.

The mushroom-like AMC (ML AMC) structure is one of the most often utilized and earliest structures in the design of

TABLE 1. Gap waveguide technology for mmWave and sub-THz applications. AMC stands for artificial magnetic conductor, GW is the gap waveguide, GGW is the groove gap waveguide, RGW is the ridge gap waveguide, SIGW is the substrate-integrated waveguide, and IMGW is the inverted microstrip gap waveguide. The TE is the transverse electric, and Q-TEM is the quasi-transverse electromagnetic.

AMC Pins	Mushroom-liked Structure		Glide-symmetry Holey Structure	
Monomode Bandwidth	★★★		★★	
Ease of Manufacturing	★★		★★★	
GW-Transmission Lines	**GGW**	**RGW**	**SIGW**	**IMGW**
Fundamental Mode	TE_{10}	Q-TEM	Q-TEM	Q-TEM
Transmission Loss	★★★	★★★	★★	★
Monomode Bandwidth	★★	★★★	★★★	★★★
Physical Size	★	★★	★★★	★★★
Ease of Manufacturing	★★	★★	★★★	★★★
Integration	★	★★	★★★	★★★
Packaging and shielding	★★★	★★★	★★	★★

★ =average;★★ = favourable; ★★★ = very favorable.

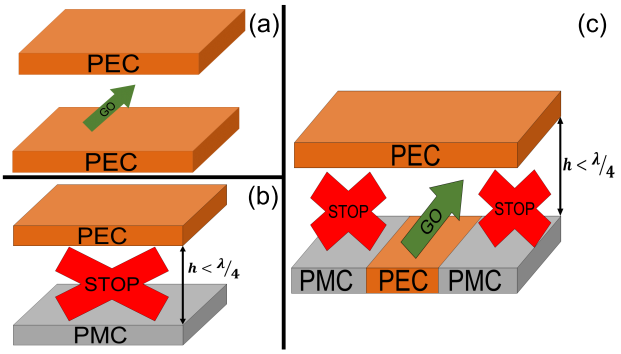

FIGURE 2. Fundamental operating principle of the gap waveguide. (a) PEC-PEC Parallel-Plate Waveguide. (b) PEC-PMC Parallel-Plate with electromagnetic wave cut-off. (c) Wave propagation concept of the gap waveguide. The green arrow with the 'GO' label indicates that electromagnetic wave propagation is permitted, while the red crosses with the 'STOP' label indicate that electromagnetic wave propagation is restricted.

GWs [10], [17]. They can be realized as substrate-integrated structures or as completely metallic structures. Fig. 3 shows multiple ML AMC structures. The mushroom structure is embedded into the substrates through metallic vias, microstrip patches, and ground, resulting in a compact design. Another low-loss technique is to use metallic AMC pins. These metallic pins come in a variety of shapes, including rectangular cubes [10], cylinders [17], cone-shaped [18], and even spring-like structures [19]. It is worth mentioning that although the geometric form of the AMC pins structures has little effect on the operational bandwidth [17], realizing the AMC pins with a varied geometry is primarily due to manufacturing considerations. On the other hand, the bandwidth performance of these pin-based structures is affected by several factors, including the pin's height, width, or diameter, the pin array's periodicity, and the air gap between the pins and the top metallic plate. Furthermore, to facilitate production, these pin structures may be created by separating them into two layers known as half-pin structures, as shown in Fig [20], [21].

Furthermore, AMC structures can be constructed employing glide-symmetric holey structures [22], [23]. The glide-symmetric holey structures, like the half-pins AMC structures, are produced utilizing two distinct layers. Unlike AMC pins, which are milled during the manufacturing process, the glide-symmetric structure requires drilling holes, making it significantly simpler to build [23]. The unit cell of the glide-symmetry holey structure and the groove gap waveguide (GGW) utilizing it are depicted in Fig. 3. The unit cell of the glide-symmetric holey structures is realized by two layers of periodic holes relocated half a period apart and separated by a minimal air gap, as seen in the figure. It should be noted that the periodicity of these glide-symmetric holey structures is roughly 2.5 times that of typical AMC pins [22]. They may make manufacturing more straightforward, but they are not appropriate for millimeter-wave (mmWave) or terahertz (THz) structures that require compact size, such as phased array design.

B. GAP WAVEGUIDE TYPES

Based on the principles above, four types of gap waveguides have been developed and implemented, known as groove gap waveguide (GGW), ridge gap waveguide (RGW), substrate integrated gap waveguide (SIGW) (sometimes also known as microstrip gap waveguide), and inverted microstrip gap waveguide (IMGW) as illustrated in Fig. 3 [12]. In general, the GGW and RGW have the same geometry as the conventional rectangular hollow waveguide and ridge waveguide, with the PEC wall replaced with AMC pins. In the case of the SIGW and IMGW, the printed circuit board (PCB) is used to construct the guiding line in a simple and cost-effective approach. The mushroom-type EBG structure is implanted into the substrate in the case of SIGW, with a stripline put between them. For the IMGW, on the other hand, the AMC pins are put underneath the PCB to package the designed microstrip lines, which aids in the elimination of undesired leakage and surface wave inside the substrates. Distinct types of gap waveguide geometries exhibit different operating modes. The benefits and drawbacks of each version are connected to manufacturing simplicity, compactness, power-handling capabilities, integrability, and loss performance, among other aspects [12]. Table. 1 summarized the performance comparison of the AMC pin structures and the four different types of the GW-technology.

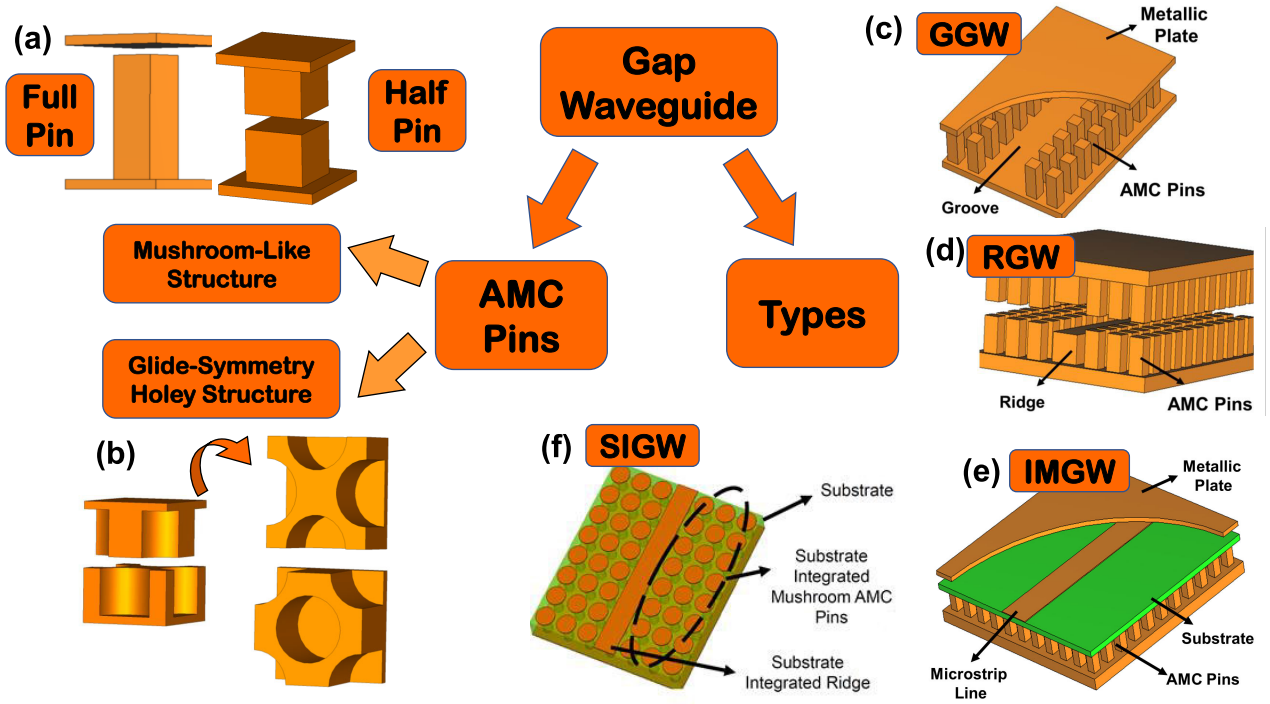

FIGURE 3. The choices of the AMC structure for the GW-technology (a) Mushroom-like structure: Full Pin and Half Pin and (b) the Glide-Symmetry Holey Structure; and different types of the GW-based transmission lines: (c) GGW, (d) RGW, (e) SIGW and (f)IMGW. The GGW is the groove gap waveguide, RGW is the ridge gap waveguide, SIGW is the substrate-integrated gap waveguide, and IMGW is the inverted microstrip gap waveguide.

III. GAP WAVEGUIDE ANTENNA

There has been an increase in interest in GW-based antennas over the past few years. To this end, numerous antenna configurations based on the GW technology have been realized. To help visualize the potential for GW technology for various antenna designs, we have classified GW-based antennas into several categories which are extensively used in mmWave and submmWave applications. These include fixed-beam slot array antennas, fixed-beam microstrip phased array antennas, leaky wave antennas, and horn antennas.

A. FIXED BEAM SLOT ARRAY ANTENNA

Over the past several years, there has been an increasing interest in developing a fixed beam array antenna based on GW technology for various applications. Several antenna configurations based on different GW technology have been successfully devised, ranging from X-band to D-band and beyond [24], [25], [26], [27]. The slot antenna has been essential in developing array antennas based on the conventional metallic waveguide because it is a straightforward implementation. Similarly, the slot antenna element has also been chosen as the primary radiating element for the numerous array antennas built employing GW technology. To disrupt current flows, the slots may be created with varied shapes and rotations and sliced into the waveguide walls. Consequently, the power traveling through the waveguide is coupled and radiated via the slots that open into free space. The first GW-based antenna was constructed by milling four slots in the RGW and operating at 13 GHz [24]. Two different feeding techniques were proposed to produce 1×4 and 2×2 array configurations, namely a linear feed and a corporate feed, respectively [24]. Another earlier design approach in designing the array antenna with a larger configuration that operates at 60 [28] was created employing the SIGW technology and later also for a 95 GHz solution based on the SIW technology [29]. However, most of these proof-of-concept antennas did not ultimately realize the benefits of the GW technology in developing mmWave array antennas since they were realized in combination with SIW structure.

In [25], a fully metallic V-band slot array antenna based on RGW with an 8×8 design is demonstrated. The array antenna comprises three layers of unconnected structures: the radiating slot layer, the GW-based cavity layer, and the RGW-based feeding layer. The suggested architecture with a larger configuration that complies with the ETSI Class II standard is subsequently proven in [30]. A similar array antenna design employing several GW-based implementation approaches has been produced, e.g., the GGW [31], [34], the SIGW [32], and the IMGW [33]. Fig. 4 illustrates several prototypes of the fixed beam slot array antenna based on different GW-technology. However, most of these slot array antennas have a bandwidth of less than 20%. Several approaches for increasing the overall bandwidth of these entirely metallic GW-based slot array antennas have been presented. It is suggested in [35] to put additional tuning pins over the cavity layer to enhance the amplitude and

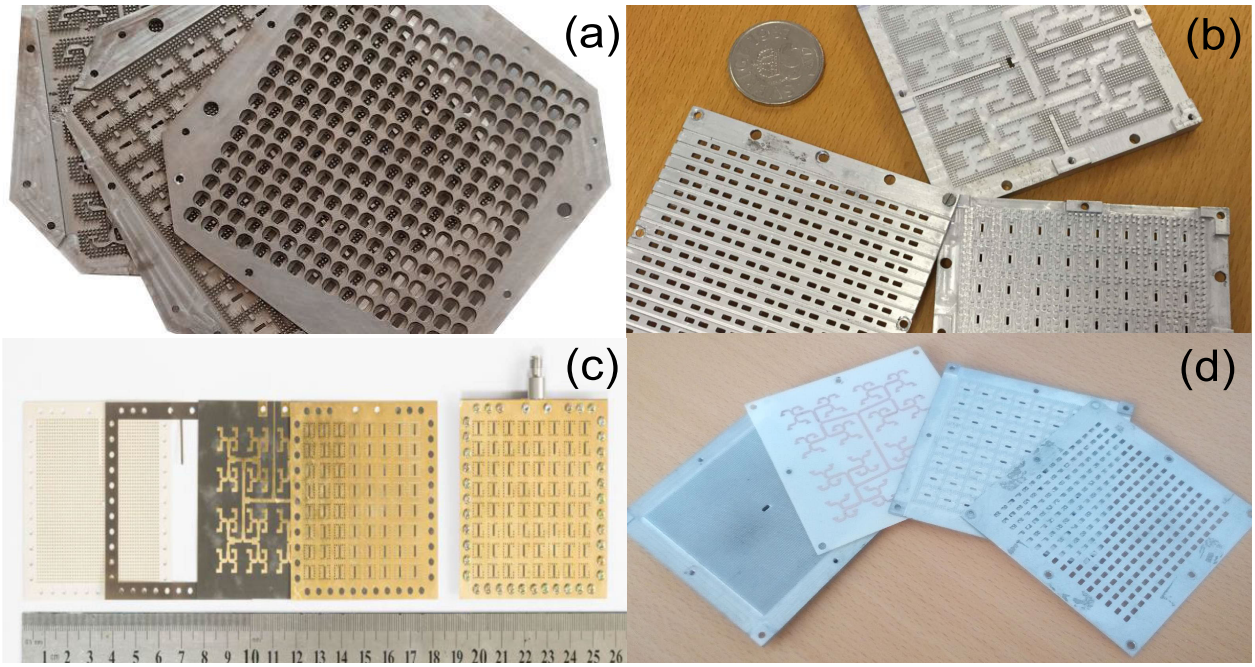

FIGURE 4. Prototypes of the fixed beam slot array antenna based on different GW-technology. (a) RGW [30], (b) GGW [31], (c) SIGW [32] and IMGW [33].

TABLE 2. Performance comparison of existing GW-based slot array antenna for mmWave and THz applications. f is the frequency band, and IBW is the fractional impedance bandwidth. AR represents the 3 dB Axial Ratio bandwidth for the circularly polarized antenna.

References	f [GHz]	Polarization	Feeding Technology	No.of Elements	IBW [%]	Peak Gain [dBi]	Measured Efficiency[%]
[25]	60	Single, Linear	RGW	8×8	14	25.8	> 65
[27]	160	Single, Linear	RGW	16×16	9.8	31.9	≈ 50
[29]	94	Single, Linear	SIW+SIGW	8×8	14.9	23.8	> 42.3
[30]	60	Single, Linear	RGW	16×16	17.6	31	> 60
[31]	60	Single, Linear	GGW	16×16	18.8	32.5	> 80
[34]	60	Single, Linear/Circular	GGW	16×16	14 (AR)	31.7 / 32.3	≈ 62.52 / 75
[32]	37.5	Single, Linear	SIGW	8×8	16	24	> 41.69
[33]	60	Single, Linear	IMGW	16×16	17	30.5	> 40
[35]	60	Single, Linear	RGW	8×8	30	27.5	> 80
[36]	28	Single, Linear	RGW	8×8	28	26.4	> 60
[37]	25	Single, Linear	RGW + GGW	8×8	53	27.7	> 60
[38]	20/30	Linear	GGW	8×8	9.8/6.67	26/29.5	> 83
[39]	20/30	Linear	GGW	4×4	9.8/6.67	26/29.5	> 68.54
[40]	30	Single, Circular	RGW	8×8	21.8 (AR)	23.5	< 85
[41]	30	Single, Circular	GGW	4×4	4.95 (AR)	22.4	> 97
[42]	30	Dual, Circular	GGW	8×8	4.95 (AR)	27	> 75
[43]	78	Dual, Circular	RGW	1×8	10.9 (AR)	14.8	> 75.9
[44]	30	Dual, Linear	GGW	8×8	4.95	27.2/27.8	$< 85/90$
[45]	30	Dual, Linear	GGW + RGW	8×8	5/5.2	28	$< 65/68$

phase of electric fields over the cavity, resulting in a 30% bandwidth increase. Another remarkably straightforward way is to change the shape of the slot from rectangular to 8-shaped, which results in a 28% increase in bandwidth performance [36]. A UWB slot array antenna based on GW technology was recently realized as an all-metallic solution. A double-step double-ridged slot structure over the radiating element and cavity surrounds the radiating element with a feeding network accomplished in a combination of RGW and E-plane GGW is used to construct a UWB GW-based array antenna with roughly 53% bandwidth [37]. Apart from the GW-array antenna with UWB performance, there is also an interest in developing dual-band performance [38], [39]. In [38], an 8×8 dual-band array antenna is realized using circular apertures and excited by two stacked cavities with varying diameters that operate at two unique frequency bands. Additionally, [39] proposes using a dual-mode GW-based coaxial resonator in conjunction with a diplexer to excite a 4×4 I-shaped slot array antenna with dual-band capabilities. Furthermore, these GW-based slot array antennas are expanded to circularly [40], [41], [42], [43] and dual-linearly polarised array antennas [44], [45]. Table. 2 summarises the performance comparisons for several published GW-based slot array antennas.

TABLE 3. Performance comparison of the microstrip antenna feed employing GW-technology for mmWave applications. *f* is the frequency band and IBW is the fractional impedance bandwidth. AR represents the 3 dB Axial Ratio bandwidth for the circularly polarized antenna. N/A indicates that the data is not available.

Antenna Elements	f [GHz]	Polarization	Feeding Technology	No.of Elements	IBW [%]	Peak Gain [dBi]	Measured Efficiency[%]
Patch [46]	60	Single, Linear	RGW	8×8	15.5	21.5	> 75
Patch [47]	12.5	Single, Linear	GGW	8×8	4	26.18	< 57.81
MED [48]	30	Single, Linear	SIGW	4×4	16.5	19.5	< 70
MED [49]	30	Dual, Linear	SIGW	1	23.4	10.5	N/A
Spiral [50]	30	Single, Circular	SIGW	2×2	34.2 (AR)	11.74	> 85
Spiral [51]	30	Single, Circular	SIGW	2×2	22.5 (AR)	12.3	57.3
Metasurface [52]	34	Single, Linear	SIGW	4×4	35.5	17.4	< 30.2
TCDA Bowtie [53]	26	Single, Linear	SIGW	8×8	55.7	21.8	≈ 40
TCDA Bowtie [54]	25	Single, Linear	SIGW	8×8	50.3	22.1	≈ 76
TCDA Spiral [55]	17	Single, Circular	SIGW	8×8	44.9 (AR)	20.9	> 30.4
MED [56]	60	Single, Linear	IMGW	16×16	19	31.7	> 71
MED [57]	94	Single, Circular	RGW + GGW	4×8	17 (AR)	23	N/A

B. FIXED BEAM MICROSTRIP ANTENNA

Unlike rectangular waveguides, the GW technology can be co-designed with a microstrip patch antenna. The benefits of combining the GW-based antenna with the microstrip antenna are that it may help to decrease feeding losses and eliminate unnecessary surface waves. Furthermore, it gives extra design flexibility in terms of antenna implementation approach, mainly producing compact-size antennas and even UWB antennas. However, because of dielectric losses, this comes with the penalty of larger losses. Fig. 5 illustrates several examples of the fabricated prototypes designed by combining microstrip antennas and the GW technology. In [46], a wideband patch antenna fed by an RGW was employed to realize an 8×8 array at 60 GHz, with an array antenna efficiency better than 75% throughout the operational bandwidth. In [47], a similar design methodology is utilized by substituting the RGW with GGW. Furthermore, the SIGW is one of the most widely used GW technologies in developing GW-based microstrip antennas. A significant number of SIGW microstrip antennas have been constructed employing various radiating components such as magneto-electric (ME) dipoles [48], [49], spiral antennas [50], [51] and metasurface antennas [52]. Furthermore, employing the tightly coupled array concept, several GW-based array antennas with UWB performance in either linear or circular polarisation have been realized [53], [54], [55]. However, even if the array antenna is developed by combining GW technology with microstrip antennas results in increased loss owing to the presence of dielectric substrates, it remains an intriguing and attractive option when compared to the usual microstrip array. The use of GW technology in conjunction with a microstrip antenna may give benefits such as surface wave suppression and improved radiation efficiency for the conventional microstrip antennas and increased bandwidth at a cheaper manufacturing cost for the metalized GW-based antennas.

C. PHASED ARRAY AND MULTIBEAM ANTENNA

Other significant classes of antenna solutions are phased array antennas (PAAs) and multibeam array antennas (MBAs), which may produce a beam in both broadside

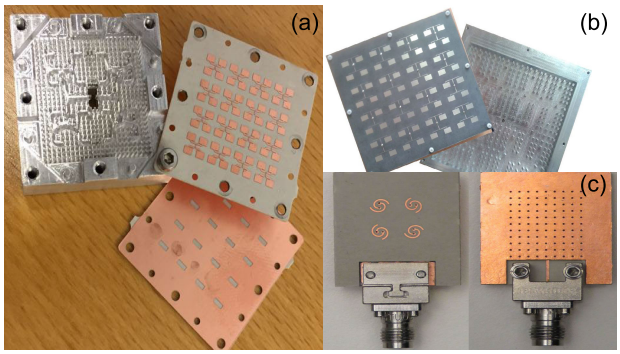

FIGURE 5. Prototypes of the microstrip antenna feed by different GW-technology. (a) RGW [46], (b) GGW [47] and (c) SIGW [50].

and other directions. In 2012, the first GW-based PAA for automotive radar applications was demonstrated at 76 GHz [58]. The suggested PAA was implemented by arranging a slot structure with a 45° inclination over the RGW and feeding it with a passive RGW phase shifter. The PAA developed has a scanning range of ±18° and a minimum gain of 32 dBi. Another GW-based PAA with 1D scanning working at 30 GHz was recently accomplished employing a 4×8 slots array and fed by an RGW-based true-time delay mechanical phase shifter [59]. The proposed PAA has a steering angle of up to 25°. In addition, [60] presents a proof of concept antenna element produced utilizing open-ended RGW to increase the bandwidth and scanning range of the GW-based PAA. Gapwaves AB, Sweden, has also shown an active PAA for 28 GHz 5G communication based on GW-technology [61]. To design an 8×8 configuration with 2D scanning, the suggested active PAA used an I-shaped slot structure as the radiating element. This suggested GW-PAA in [61] was later upgraded and optimized to have a better scanning performance and output EIRP by making the GW-PAA considerably compact and improving the microwave electronics chain to obtain an E-plane scanning of ±60° with an EIRP of 60 dBm, as shown in [62]. Moreover, a 16×16 GW-PAA with slant polarized is realized with the 45° slant slot for 5G mmWave application with 2D scanning capability is presented in [63]. It is worth

noting that all of these GW-PAA are designed employing the RGW.

Furthermore, various GW-based multibeam array antennas have been suggested. These multibeam array antennas are often designed to work with the Butler matrix (BM) beamforming network, which supports beamforming over 1D- and 2D-scanning spatial directions. For example, a 2×2 magneto-electric dipole (MED) antennas were fed by the SIGW BM to construct a 30 GHz multibeam array antenna that supports 2D scanning for 5G applications [64]. In addition, the SIGW-based BM is also used to feed other antennas like as semi-log periodic arrays [65] and dielectric resonator antenna (DRA) [66] in realizing a multibeam array antenna. These multibeam array antennas are also accomplished by designing the beamforming network employing RGW [67], GGW [68], [69], [70], and IMGW [71] to feed various antenna configurations. In addition to the BM, the Luneburg Lens is a common alternative beamforming network used to realize the multi-beam antenna [72], [73]. Recently, several gap waveguide-based multibeam antennas with V-band Geodesic Luneburg lenses have been realized [72], [73]. The utilization of the gap-waveguide based on glide-symmetry holey EBG structure enabled these geodesic Luneburg Lenses to be realized as a multi-layers structure, significantly reducing the fabrication complexity while eliminating the unwanted radiation leakage between the feed ports and the multi-layers structure. The proposed solution demonstrates a broad beam coverage and high radiation efficiency. Table. 4 shows the performance comparison of several GW-based PAAs and multibeam array antennas that have been demonstrated.

D. LEAKY-WAVE ANTENNA

Another type of antenna that has gained substantial interest in the mmWave and THz band is the leaky-wave antenna (LWA), which employs a guiding structure that facilitates wave propagation over the length of the structure, with the wave radiating continuously along the structure [74]. This sort of antenna is typically fed from one end, prompting the wave to flow along the structure's axis, forming a fan beam at either the broadside or a conical beam that radiates at a particular scanning angle concerning the guiding structure's axis [74]. The long slots array antenna fed by a quasi-TEM H-plane horn created employing the RGW is used to demonstrate the first GW-based LWA [75]. In that work, the RGW horn provides a uniform co-polarized electric field along the waveguide structure. The slots are cut over the top PEC layer of the RGW to leak the radiation; however, the proposed design resulted in significant grating lobes. To improve the LWA's radiation performance, a dielectric slab and horn-shaped corrugation are mounted on the top of the radiating slots. In [76], an identical RGW H-plane horn demonstrated in [75] is used as a launcher for feeding the metal strip grating (MSG) LWA. This MSG LWA is created by combining 35 metallic strips with perforated holes. Furthermore, for E-band applications, a wideband and high gain LWA is realized by employing the tapered slot array antenna fed by the SIGW [77]. To improve the gain performance, a Y-junction power divider feeds two rows of the LWA, resulting in an additional 3 dB gain performance.

A simple alternative LWA utilizing the GGW was proposed for X-band applications and was presented in [78]. The proposed LWA is implemented by correctly identifying the GGW lengths. Theoretically, the periodic AMC pins in the GW are intended to inhibit electromagnetic wave leakages. However, for the developed LWA to radiate, significant leakage of the EM waves is necessary. To accomplish this, the number of AMC pins on the lateral sides of the GGW is suitably chosen. The study recommended employing three rows of AMC pins over one side of the GGW to avoid EM leakage and one row of AMC pins over the lateral side of the GGW to ensure sufficient EM leakage for radiation. This GGW leakage radiation may then serve as a basic LWA. Furthermore, to improve radiation performance, the height of the pins for the one-row lateral sides should be decreased, which guarantees higher EM wave leaking. The proposed concept is later employed in numerous LWA designs [79], [80]. However, instead of AMC pins, glide-symmetry holey structures are used as AMC structures for these LWAs. The LWA is dispersive, which means that the direction of the radiating beam varies with frequency. However, for some applications, such as point-to-point communication, the dispersive effects become detrimental. As a result, a holey metasurface prism is added to the proposed GGW LWA to mitigate the dispersive effects. This reduces the beam direction deviation over the frequency to as little as 1° [79]. A circularly polarised LWA is also obtained by constructing a 45° inclined hexagonal patch antenna and feeding it with GGW [81]. Two rows of these CP patches are positioned above the GGW and are excited by the coupling slots on top of the GGW. Table. 5 compares the performance of several published LWAs based on GW technology. It should be noted that most of these LWAs are accomplished via RGW, GGW, and SIGW. To the authors' knowledge, no LWA has been built employing IMGW until now.

E. HORN ANTENNA

Horn antennas have been widely employed for microwave applications for the past 70 years as wideband, high gain, and low loss radiating elements. Typically, conventional horn antennas are fed via a waveguide, which is normally built from PEC. However, fabricating these horn antennas could be complex and challenging, particularly at higher frequencies, because of the compact dimensions, manufacturing tolerances, and electrical contact requirements. These horn antennas may be designed employing GW technology too. Fig. 6 illustrates the evolution of the horn antennas designed based on the GW technology.

Indeed, among the first proof-of-concept antenna based on GW technology introduced by *Kildal's group* in the year 2014 was created utilizing a horn antenna [82]. However, the

TABLE 4. Performance comparison of the GW-based Phased-Array and Multibeam Array Antenna. PAA is the phased array antenna and MBA is the multibeam array antenna. *f* is the frequency band, and IBW is the fractional impedance bandwidth. LHCP is defined as a left-handed circularly polarized antenna. N/A indicates that the data is not available.

Antenna Elements	f [GHz]	Polarization	Feeding Technology	No.of Elements	IBW [%]	Scanning Range	Gain/EIRP [dBi/dBm]	Measured Efficiency[%]
PAA								
Slot [58]	76	Single Linear	RGW	16×10	3.9	$\pm 18^\circ$ (E-Plane)	32	N/A
Slot [59]	30	Single Linear	RGW	4×8	3.3	$\pm 25^\circ$ (E-Plane)	20	≤ 90
1D open--ended RGW [60]	100	Single Linear	RGW	1×19	21	$\pm 40^\circ$ (H-Plane)	N/A	≥ 91
Slot [61]	28	Single Linear	RGW	8×8	10.7	$\pm 45^\circ / \pm 10^\circ$ (E/H-Plane)	52	N/A
Slot [62]	28	Single Linear	RGW	8×8	10.7	$\pm 60^\circ$ (E-Plane)	60 65	N/A N/A
45° Slant Slot [63]	28	Single Slant	RGW	16×16	10.7	$\pm 60^\circ / \pm 10^\circ$ (E/H-Plane)	65	N/A
MAA								
ME-Dipole [64]	30	Single Linear	SIGW	2×2	20	$\pm 35^\circ / \pm 35^\circ$ (E/H-Plane)	10.3	≈ 84
semi-log arrays [65]	30	Single Linear	SIGW	1×4	21.25	$\pm 35^\circ$ (N/A)	10.3	≥ 78
DRA [66]	31	Single Linear	SIGW	1×4	11.5	$\pm 45^\circ$ (N/A)	≥ 9.27	N/A
Endfire-Dipole [67]	28	Single Linear	RGW	1×4	24.54	$\pm 42^\circ$ (H-Plane)	≤ 13.94	≤ 91
Septum Antenna [68]	85	Single Circular	GGW	1×4	17.6	$\pm 28^\circ$ (LHCP)	≤ 15.29	≤ 89
Endfire Tapered Slot [69]	100	Single Circular	GGW	2×2	38.7	$\pm 25^\circ$ (LHCP)	≤ 12.8	≤ 92.5
Slot [70]	28	Single Linear	GGW	4×4	15.65	$\pm 37^\circ$ (E-Plane)	≥ 14.46	≥ 97
Horn [71]	30	Single Linear	IMGW	1×4	16.7	$\pm 42^\circ$ (H-Plane)	≤ 12	≈ 70
Geodesic Lens [72]	59	Single	GGW	Single	10.2	$\pm 55^\circ$ (H-Plane)	≥ 16.5	≈ 75
Water-drop Lens [73]	59	Single Linear	GGW	1×4	10.2	$\pm 30^\circ / \pm 55^\circ$ (E/H-Plane)	≤ 22.5	N/A

TABLE 5. Performance comparison of the GW-based Leaky-wave Antenna. *f* is the frequency band and IBW is the fractional impedance bandwidth. N/A indicates that the data is not available.

Antenna Elements	f [GHz]	Polarization	Feeding Technology	IBW [%]	Beam Direction	Gain [dBi]	Measured Efficiency[%]
[75]	27.5	Linear	RGW	10.9	$+10 \pm 7^\circ$	18.5	89
[76]	28.5	Linear	RGW	7.02	$-20 \pm 5^\circ$	24	89
[77]	59	Linear	SIGW	27	$-25 \pm 10^\circ$	17.67	≥ 89
[78]	10.5	Linear	GGW	19.05	$+45 \pm 3^\circ$	19	90
[79]	27	Linear	GGW	14.8	$+55 \pm 3^\circ$	16	≥ 95
[80]	60	Linear	GGW	11	$+44 \pm 3^\circ$	17	≥ 90
[81]	31.5	Circular	RGW	9.52	$\pm 45^\circ$	17	N/A

benefits of GW technology in the design of horn antennas were not fully demonstrated then because it was solely used to create a low-loss power divider for feeding the array of conventional horn antennas. Later on, an integrated quasi-TEM horn based on RGW technology is described [76] as the launcher for the leaky-wave antenna. The designed RGW H-plane horn included an AMC pin replacing the traditional H-plane horn's PEC side wall. Two benefits resulted from this design method: the tapering field distribution throughout the width of the standard H-plane horn is addressed by AMC pins, and the horn may be manufactured as two distinct metal plates and cascaded afterward without any electrical connection issues [76]. The study provided the essential design concept for a variety of GW-based horn antennas that were designed employing different GW technologies such as SIGW [83] and GGW [84], [86]. It is worth noting that most of these reported works are concentrated in 2D planar designs. As a result of the limitation of design flexibility in these 2D planar structures, all of these studies are reported only for H-plane horns. The work presented in [85], proposed another designed approach that makes use of the benefits of the GW technology by constructing a 3D dual polarisation pyramidal horn antenna fed by 3-D GW orthomode transducer (OMT) employing SIGW-technology. The designed 3D pyramidal horn with OMT provides a bandwidth of around 28% at 31 GHz. Thus, unlike traditional horn antennas, which require sophisticated manufacturing to ensure the electrical connection, the GW-based horn antenna

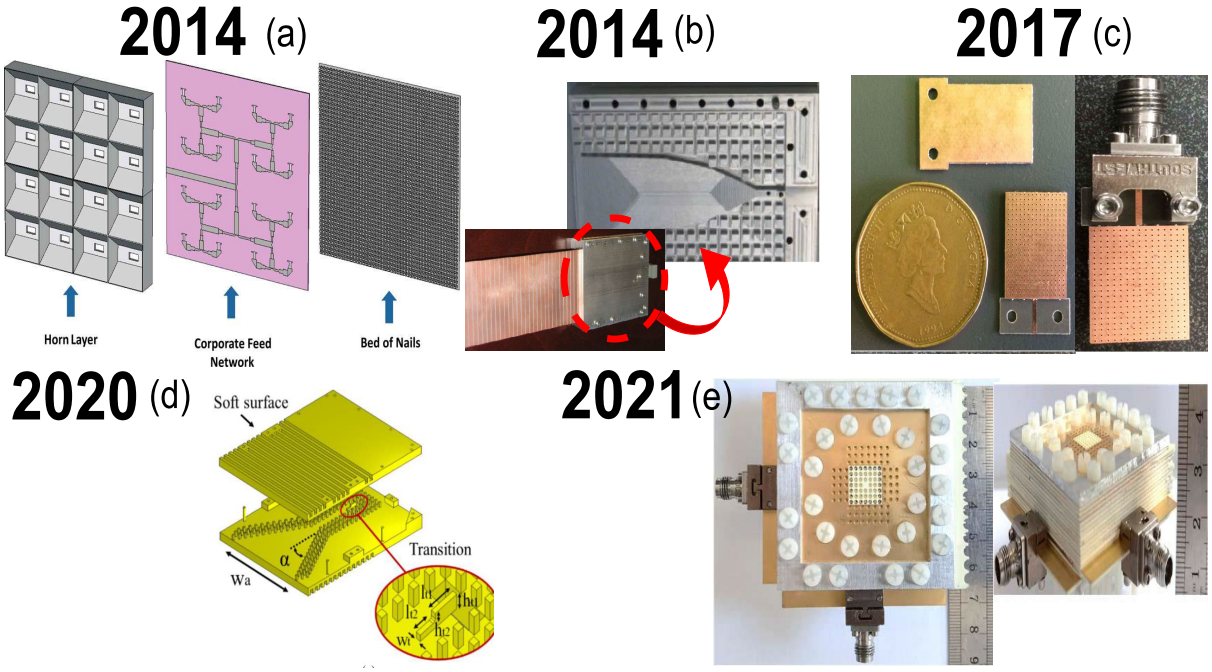

FIGURE 6. The technological evolution of the gap waveguide based horn antennas. (a) An array of horn antennas fed by IMGW [82]; (b)RGW-based quasi-TEM H-plane horn launcher for leaky-wave antenna [76]; (c) SIGW-based H-plane horn antenna [83]; (d) GGW-based horn antenna [84]; and (e) 3D dual-polarized GGW-based horn antenna fed by OMT [85].

may be realized by employing a much simpler manner. The GW-based horn may be constructed by creating layered structures and cascading these afterward without having to worry about electrical connections, resulting in substantial cost savings.

IV. GW-BASED PASSIVE CIRCUIT

Owing to the resemblance between GW structures and conventional transmission-line structures such as rectangular waveguides, SIW, or even coplanar waveguides, depending on the GW technology employed, it has garnered considerable interest in realizing various GW-based passive circuits. Suppose a high Q-factor passive circuit is needed. In that case, the GGW may be utilized to produce such a passive circuit since its loss performance is equivalent to that of a conventional rectangular waveguide.

A. BEAMFORMING CIRCUIT

The beamforming circuit is essential to the design of fixed beam array, phased array, and multibeam array antennas. These circuits may be power dividers, couplers, or phase shifters. The power divider and directional couplers are used to divide or combine the EM power to the different ports. Fig. 7 shows several prototypes of the GW-based power divider or coupler. These power dividers or couplers, like the GW-based antenna, may be developed based on different types of the GW [31], [56], [57], [65].

Similarly to the design of the power divider employing conventional transmission lines, it is critical to provide adequate isolation between ports and minimal insertion loss

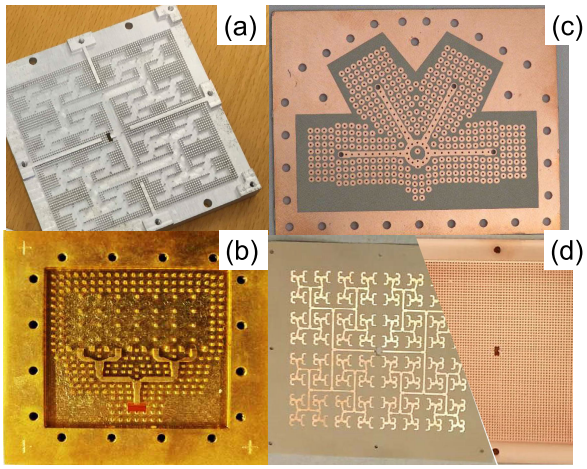

FIGURE 7. Fabricated prototypes of the GW-based power dividers or couplers. (a) A corporate-feed network formed by GGW power divider [31], (b) an RGW power divider [57], (c) a SIGW coupler [65] and (d) a Ccrporate-feed network form by IMGW power divider [56].

across the working bandwidth while designing the GW-based power divider. Fig. 8 illustrate the T-junction power divider based on GGW and RGW that is commonly employed in the design of the GW-based array antenna. As can be seen, both the GGW and RGW power dividers have an inductive post, the main purpose of which is to improve the reflection coefficient from the ports. Furthermore, in the case of GGW, an extra matching pin is positioned near the power divider's T-junction and is utilized for impedance matching over a wider bandwidth. The height of this tuning pin is critical to the power divider's bandwidth performance [31]. In the

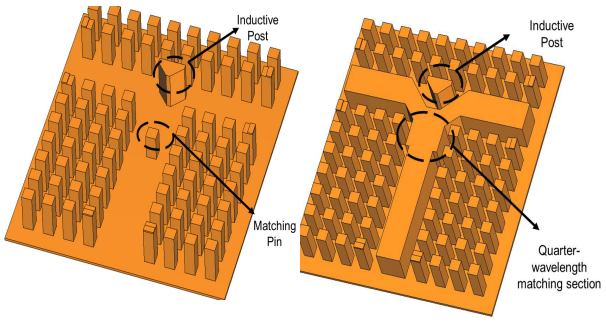

FIGURE 8. Configuration of the T-junction power divider based on GGW and RGW.

case of RGW, a quarter-wavelength ridge is used to enhance matching [30]. These parameters may be tuned to provide a GW-based power divider with wideband and excellent isolation. Apart from the design rules mentioned above, one should note that the bandwidth performance of a GW-based power divider is highly dependent on the GW types. Since the GGW's working mode is identical to a standard metallic waveguide, the bandwidth performance is often substantially narrower than other GW. If wideband or even UWB performance is needed, a GW-based power divider developed employing RGW, SIGW, or IMGW should be considered. This is primarily because they operate in quasi-TEM mode, and their cut-off frequencies are primarily determined by the operational bandwidth of the AMC pins, which are often broadband. This also becomes clear by inspecting Tables. 2 and 3, where array antennas based on GGW often have substantially narrower bandwidth than array antennas based on RGW, SIGW, and IMGW. In general, the majority of power dividers evenly split the input power to the output port. An unequal power divider based on GW technology, on the other hand, can be implemented instead [87]. These unequal power dividers are typically employed to lower the side lobes level of the array antenna [52], [88]. Furthermore, the GW technology has been used to design several other forms of power dividers or couplers, such as the Gysel power divider, rat-race couplers, and 3 dB hybrid couplers [65], [89], [90], [91], [92], [93].

Another essential microwave component for beamforming is the phase shifter. RGW was used to construct the first GW-based phased shifter at 76 GHz [58]. The suggested phase shifter features a phase shift of more than 180 degrees and an insertion loss of less than 1.5 dB. Another GGW-based phase shifter was created by putting a small layer of substrates into the GGW to achieve a 90-degree phase shift [94]. A similar design method is used in building a V-band phase shifter [95]. However, instead of employing a thin substrate layer to achieve the phase shift, the work proposes to create the phase shift by carefully arranging the metallic pins [95]. Moreover, a wideband phased shifter is realized using the RGW with a wideband performance [96] Other reconfigurable phase shifters, either by mechanical tuning [59], [97] or using liquid crystal [98], have recently been suggested.

Furthermore, numerous butler matrix (BM) beamforming networks have been constructed by integrating this GW-based coupler and phase shifter [64], [65], [67], [68], [70], [71], [99], [100]. Fig. 9 illustrates several fabricated prototypes of the BM beamforming networks, which are designed employing different GW-technology. The first GW-based BM was suggested in 2018 utilizing SIGW-technology [64]. In this study, a 4×4 BM operating at 30 GHz with approximately 20% operational bandwidth was developed for use in a 5G small cell base station. Four 90-degree GW-based hybrid couplers were used in the BM. Moreover, a BM with better loss performance was built for monopulse radar applications at 94 GHz utilizing GGW. They have an IL of around 0.8 dB. Subsequently, several BM realized employing IMGW [71] and RGW [67] were presented. Furthermore, an alternative lens-based beamforming network based on GW technology was quantitatively investigated [101], [102]. Recently, these lens-based beamforming networks have been realized and experimentally verified [72], [73], [103]. Fig. 10 illustrate several prototypes of the GW-based lens-types beamforming structure for both fixed and multi-beam antennas.

B. FILTERS AND DIPLEXERS

The filter is another essential passive circuit that has piqued the interest of researchers owing to the increasing demand for wireless communication applications. Fig. 11 shows several filter topologies developed by employing various versions of the GW technology. These GW-based filter architectures may be created using traditional microstrip filters, such as parallel-coupled [104] and end-coupled [105] filters for IMGW and SIGW-based filters, or metallic waveguide filters, such as coupled-resonator filters [106] for SIGW, RGW, and GGW. The IMGW was used to construct the first GW-based filter; this filter utilized the conventional microstrip parallel-coupled technique and placed it between the metallic AMC pins and the PEC metallic plate for Ku-band application [104]. A fourth-order bandpass filter for V-band applications was created employing a similar design approach [105]. However, the end-coupled mechanism is used in the filter design instead of the parallel-coupled design. Moreover, numerous filters have been developed employing SIGW [107], [108], [109], [110]. However, these IMGW and SIGW filters often have higher insertion loss due to the presence of the dielectric substrate. To achieve the lower loss in GW-based filters, the GGW and RGW are often used [106], [111], [112], [113], [114], [115]. These GW-based filters have been realized for various frequency bands spanning from X-band to D-band [115]. Furthermore, to make the GW-based filter more compact, it was recommended to develop the filter employing the slow-wave GW [116], [117]. In [116], a slow wave SIGW filter is accomplished with a size reduction of up to 62% compared to a SIGW filter developed employing the

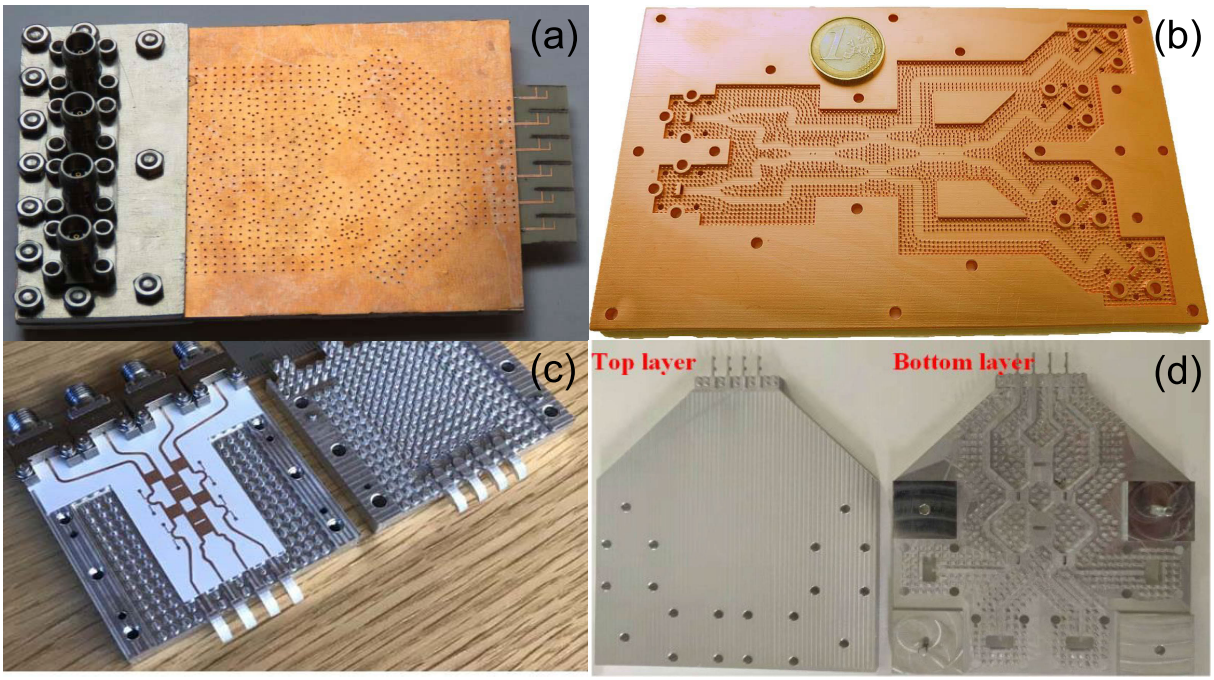

FIGURE 9. Manufactured prototype of the Butler Matrix (BM) beamforming network based on different versions of the GW technology. (a) SIGW BM [65], (b) GGW-based BM [99], (c) IMGW BM [71] and (d) RGW BM [67].

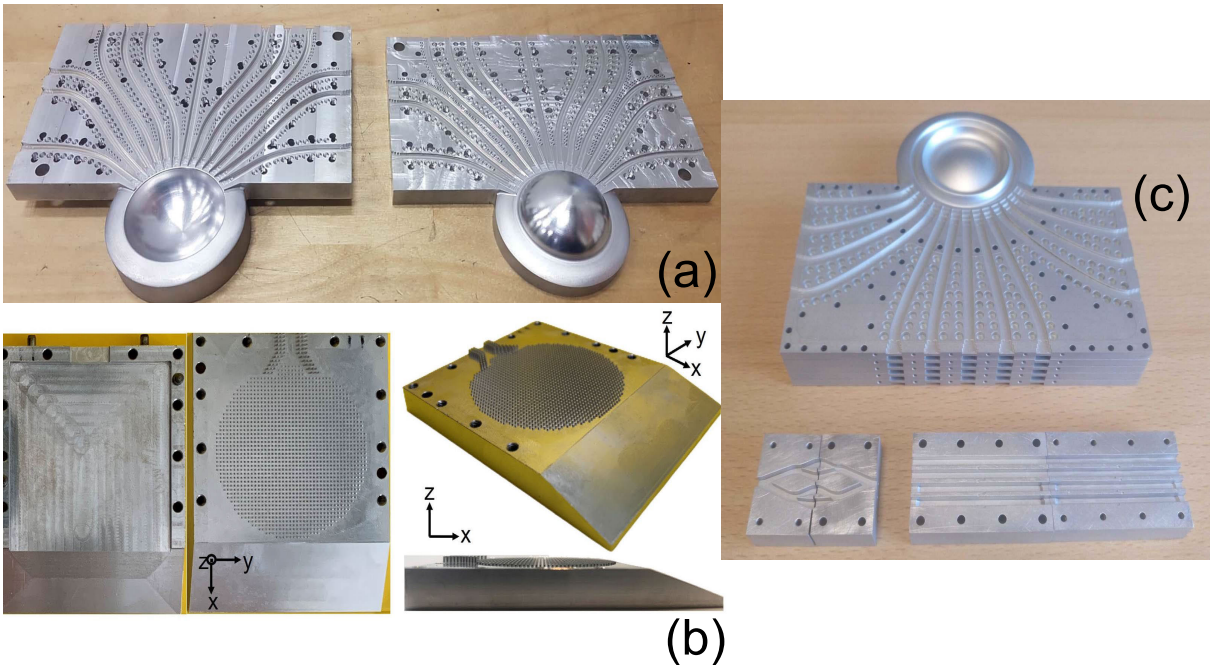

FIGURE 10. Manufactured Luneburg Lens beamforming network prototype based on GW technology. (a) 1D-Multibeam Antenna based on Luneburg Lens [72], (b) Fixed-beam Luneburg Lens Antenna [103] and (c)2D-Multibeam Antenna based on Luneburg Lens Antenna [73].

conventional technique. A constructed GGW-based filter using the likewise slow-wave idea exhibits miniaturization up to 57.1% [117]. Alternately, the miniaturization of the GGW filter can also be achieved by filter employing horizontally polarised GGW [118]. In addition, multi-layer GGW-based filters may be implemented utilizing the direct coupled approach to reduce the size of the filters [119], [120]. In addition, a GW-based bandpass frequency selective surface filtering radome has been demonstrated in [121]. The user of the GW in the FSS radome design has greatly enhanced the filtering response of the FSS, especially at the rejection band.

Furthermore, the GW-based filter design concept may be extended to diplexers. An X-band diplexer is constructed utilizing two GGW fourth-order Chebyshev filters, one for

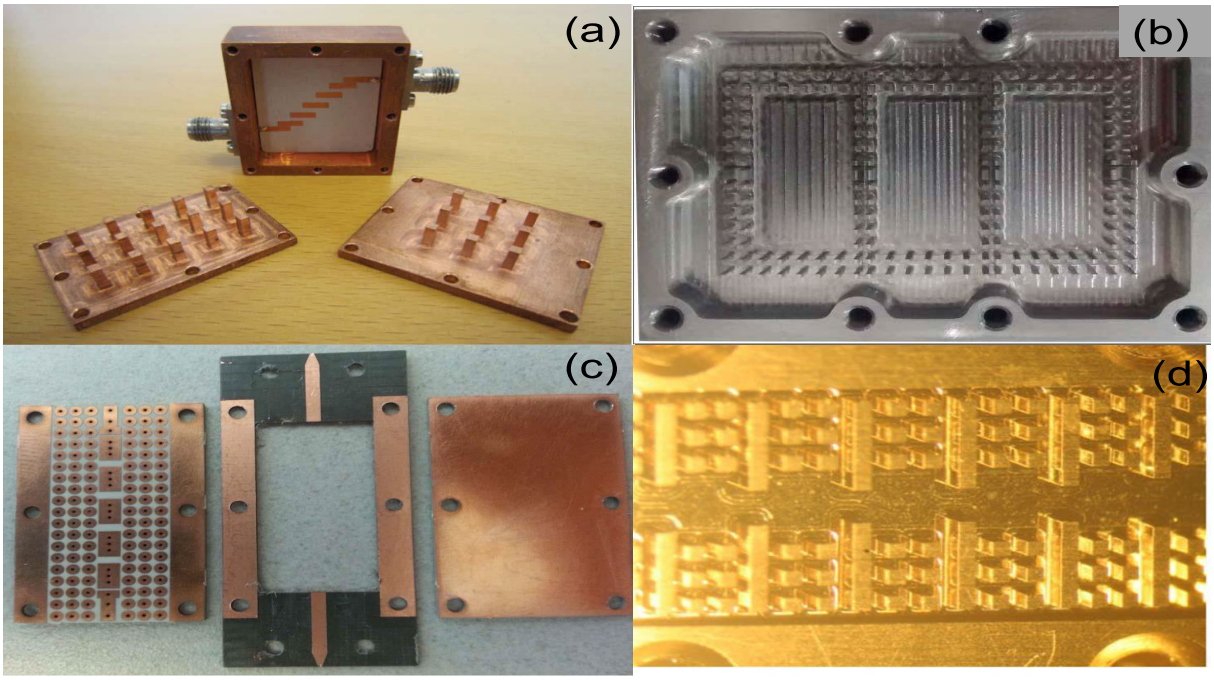

FIGURE 11. Photograph of the fabricated GW-based filters. (a) IMGW parallel-coupled filter [104], (b) GGW coupled-resonator filter [106], (c) SIGW end-coupled filter [107] and (d) GGW iris-window filter [115].

transmission and one for reception [122]. The suggested diplexer has a bandstop attenuation of more than 20 dB and an insertion loss of roughly 1.5 dB in the passband frequency. This concept has been further developed for several frequency bands such as Ku-band [123], Ka-band [124], and E-band diplexer [125]. Moreover, a Ka-band diplexer has been realized employing the IMGW filter [126]. The proposed diplexer demonstrates an insertion loss of around 2 dB in the passband and attenuation of more than 20 dB in the stopband. Table 6 shows the performance comparison of several GW-based filters and diplexers that have been demonstrated. Fig. 12 illustrates a prototype Ka-band diplexer realized utilizing the GGW and integrated with the array antenna. Based on these findings, we may conclude that GW technology is a promising solution for developing high-quality-factor filters and diplexers.

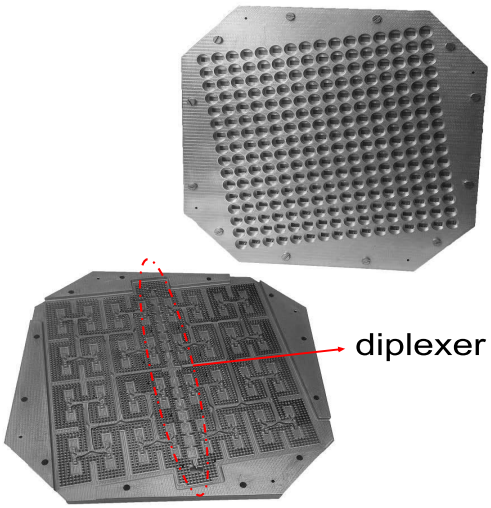

FIGURE 12. Photograph of the Ka-band GGW-diplexer integrated with the array antenna [124].

V. GAP WAVEGUIDE FOR PACKAGING AND INTEGRATION

Packaging is another important facet of mmWave and THz technologies since various components such as RF circuits, analog, digital, and power supply circuits will be packaged in a single module. Conventionally, most active MMICs are put on a dielectric substrate and interconnected to other electric circuits, such as power and digital control, through microstrip lines and connecting vias. Metallic box lids are often utilized to shield high-speed electronic circuitry from the hostile environment. However, because of the cavities formed between the circuit and the lids, this metallic lid risks forming undesired resonances, resulting in a significant degradation in circuit performance [127].

The use of GW for mmWave and terahertz packaging has sparked considerable interest in electromagnetic packaging, which can potentially address the issues above. It was numerically and experimentally proven in [128] and [129] that by packing a microstrip line over the GW (creating an IMGW), the cavity mode generated between the conventional metallic lid and the high-speed interconnected circuit may be effectively suppressed. An EMC radiation emission measurement of a working high-speed circuit package by the GW is used to validate the proposed design principle further [130]. From the measurement findings, the measured electric field of the high-speed circuit packaged with the

TABLE 6. Performance comparison of the GW-based filters and diplexers. f is the frequency band, and IBW is the fractional impedance bandwidth. IL and RL denote the insertion loss and the return loss, respectively.

References	f [GHz]	Filters Topology	Filter Order	Feeding Technology	IBW [%]	IL [dB]	RL [dB]
Filters							
[104]	15	Parallel-coupled	5	IMGW	10.7	1.5	≤ -15.3
[105]	60	End-coupled	4	IMGW	3.33	1.6	≤ -25
[106]	14	Coupled-resonator	3	GGW	4.17	≤ 1	≥ -20
[107]	30	End-coupled	5	SIGW	3.3	≥ 0.8	≤ -20
[107]	30	Coupled-resonator	3	SIGW	3.3	≥ 1	≤ -19
[108]	14.63	Coupled-resonator	5	SIGW	5.5	1.35	≤ -10
[109]	24.78	Coupled-resonator	4	SIGW	4.68	2.1	≤ -12
[110]	29.5	Coupled-resonator	3	SIGW	3	1.5	≤ -18
[111]	31.5	Coupled-resonator	4	RGW	1.6	≤ 0.45	≤ -20
[113]	33.5	Iris window	4	GGW	12.12	0.2	≤ -20
[114]	35.5	Cross-coupled	4	GGW	1.4	0.5	≤ -21
[115]	145	Iris window	6	GGW	4.17	≥ 2.2	≤ -20
[116]	11.8/18	Slow-wave	2	SIGW	3.2/8.3	1.29/1.19	≤ -30
[117]	11.87	Slow-wave	6	GGW	3.88	0.5	≤ -18
[118]	30	Comline	4	GGW	1.7	≥ 1.67	≤ -20
[119]	35	Multi-layer Cavity Resonator	3	GGW	1	≥ 1.5	≤ -10
[120]	73.65	Multi-layer Cavity Resonator	4	GGW	8	≥ 0.45	≤ -10
Diplexers							
[122]	13.7/14	Coupled-resonator	4	GGW	1.46	1.5	≤ -15
[123]	14/15.5	Coupled-resonator	4	GGW	3.5	≤ 0.8	≤ -10
[124]	28.21/29.21	Iris window	7	GGW	2.3	≥ 0.9	≤ -13
[125]	59.5/62.5	Iris window	5	GGW	1.7	≥ 0.8	≤ -13.6
[126]	24/28	End-coupled	5	IMGW	4.1	≥ 1.1	≤ -10

traditional metallic lid is more than 100 dBuV/m from $6.8 - 13.2$ GHz and drops to less than 90 dBuV/m when packaged with the GW. Furthermore, GW technology may provide excellent isolation performance between RF circuits when these RF circuits are placed in the same GW module. It was proved in [131] that when two separate RF chains consisting of power amplifier modules are packaged in a single GW module, the isolation between them is more than 60 dB.

Another critical aspect of the GW-packaging technology is its compatibility with conventional transmission lines such as microstrip, coplanar waveguide (CPW), SIW, and hollow waveguide. The primary reason is that MMICs are often mounted above the substrate, with their inputs and outputs implemented employing a 50Ω microstrip or CPW transmission line. On the other hand, several components and devices working in the mmWave and THz bands have been created utilizing SIW and WG technologies. For example, the standardized rectangular waveguide in the mmWave band is often used to realize several different measuring equipment. A seamless transition from GW to these transmission lines is critical to ensure that GW technology is compatible with other traditional transmission lines. Numerous studies have shown a good transition between various GW technologies and traditional transmission lines operating at different frequencies [132], [133], [134], [135]. The coupling approach is proposed in [132], to produce a wideband and low-loss transition between a microstrip line and an RGW. Because the RGW's dominant mode is the quasi-TEM mode, which is identical to the dominant mode of the microstrip line, the coupling between RGW and the microstrip line may be accomplished by tapering down the width of the ridge for RGW to the width of the microstrip line. Over the range of 25 to 40 GHz, this results in a transition with $S_{11} \leq -15$ dB and insertion loss of $\approx$ 0.5 dB. This coupling approach is subsequently utilized in [133] to create a transition between a microstrip line and a GGW. However, the transition design should be more sophisticated since the GGW's operating mode differs from that of the microstrip line. A quarter-wavelength depth resonant cavity was employed to link energy from the microstrip line to the GGW in the proposed transition. The results show a smooth transition for $S_{11} \leq -13$ dB from $55 - 71$ GHz and an insertion loss of roughly 0.45 dB. An alternative approach based on the Chebyshev transformer is presented in [134] to realize the transition between the microstrip line to the GGW for W-band applications. Furthermore, in the case of SIGW and IMGW, no special transition is required since the dominant operating mode of these GW is a quasi-TEM mode and can be implemented employing the microstrip line. However, the transition from SIGW or IMGW is mainly aimed at producing the smooth transition with wideband impedance matching for 50Ω termination like the conventional microstrip line design [82], [136]. On the other hand, various GW-based antennas [30], [31] have demonstrated the transition from GW to the conventional rectangular waveguide. Similarly to the previous GW-microstrip line transition design, the coupling method is considered in most of the transition designs from GW to the waveguide. For example, a probe realized employing a ridge is used to couple the energy from a standard rectangular waveguide to the RGW [30] and the GGW [31].

Furthermore, to demonstrate the benefit of employing GW technology for packaging, some studies have shown the

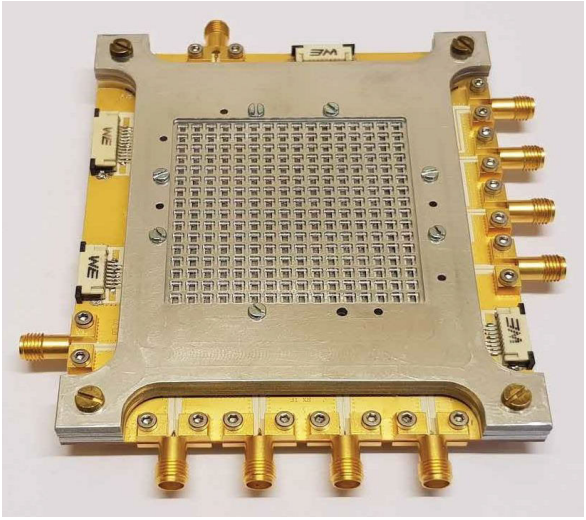

FIGURE 13. Photograph of the compact front-end for full-duplex E-band backhauling communication design and packaged employing GW-technology [139].

complete integration and packaging of active and passive RF components that are designed with other transmission lines employing GW technology. In [137] and [138], a power amplifier module is packaged utilizing RGW and wire bonding, eliminating the need for a substrate. Moreover, as shown in Fig. 13, a compact integrated full duplex RFFE for point-to-point backhaul links operating in the E-band has been created utilizing GW-technology [139]. GW technology combined numerous active and passive components in this study. The array antenna is initially built utilizing RGW as the first three metallic layers, and a GGW-based diplexer is afterward incorporated in the structure's layer 4. Additionally, layer 4 had a transition design to couple the energy from the microstrip line, which included an active transceiver module positioned underneath layer 4. Therefore, the proposed integrated RFFE module presented in [139], has demonstrated the mechanical flexibility and enormous potential of GW technology in system integration and packaging of high complexity. A similar integration and packaging concept is later used in [61], [62], and [63] to realize a high-performance active GW-PAA for mmWave 5G applications.

VI. FABRICATION TECHNOLOGIES FOR GAP WAVEGUIDE DEVICES

The manufacturing methodologies of GW-based structures are commonly categorized into two categories according to how the AMC pins are constructed. The first type is SIGW, which has a relatively simple manufacturing method that is equivalent to the fabrication process of a conventional microstrip technology. Another category is GW which is made entirely of metal. Due to the intricate pattern and physical dimensions of the AMC pins structure, the production process for the all-metallic GW is much more complicated, particularly when the operating frequencies are increased. This section overviews the current manufacturing techniques used to produce the all-metallic GW. Table. 7 shows four manufacturing technologies that are commonly employed for the fabrication of GW-based components. These manufacturing technologies include computer numerical control (CNC) milling technology, die-sink electric discharge machining (EDM), 3D-printing technique, and chemical metallic etching.

The CNC milling technology is one of the most commonly used manufacturing technologies that is currently used for the production of GW-based components [25], [26], [140]. In this manufacturing process, computerized controls and rotating multi-point cutting tools are used to gradually eliminate undesirable metallic parts from the metallic block and generate a pattern that meets the design's specifications. This CNC machining technology is a mature fabrication technology that could provide high manufacturing accuracy at both mmWave and sub-THz frequencies. Nevertheless, this CNC milling technique is relatively time-consuming, and for large-scale manufacturing required by the industry, this CNC milling can be very costly. This manufacturing cost is especially critical as the frequency increased to sub-THz, which required higher fabrication accuracy.

Alternatively, die-sink electric discharge machining (EDM) is suggested as a preferable option for large-scale production [30], [141]. In EDM, a desired pattern is produced by removing material using high-energy electrical discharges between two conductive materials (a workpiece and an electrode) separated by a dielectric fluid [142], [143]. The electrode is made up of the negative of the desired design, and the high-intensity sparks cause this pattern to produce a footprint on the workpiece's surface [142]. Due to their high electrical and thermal conductivity and melting temperature, graphite or copper alloys are commonly used for the electrode [142], [143]. Thermal and electrical conductivities of the workpiece are the most important variables that influence the manufacturability and quality of the final product when utilizing the EDM process because they determine how the material heats up and vaporizes [142]. Although EDM manufacturing is preferable for large-scale manufacturing, it is not as widely available as CNC milling. Furthermore, the implementation of production at sub-THz GW components necessitated additional research. To the authors' knowledge, no works for sub-THz GW components produced utilizing EDM technology have been presented.

In recent years, 3D printing for antenna and microwave component fabrication has received an enormous amount of attention as an alternative and adaptable manufacturing technique for high-frequency applications [144], [145]. The primary advantages of this approach are that it enables low-cost prototyping and the manufacture of complex 3D objects. There are two kinds of 3-D printing technology, i.e., metal-based and polymer-based with metallic plating. The majority of currently reported 3D-printed GW-based devices are created using polymer-based 3D printing, with

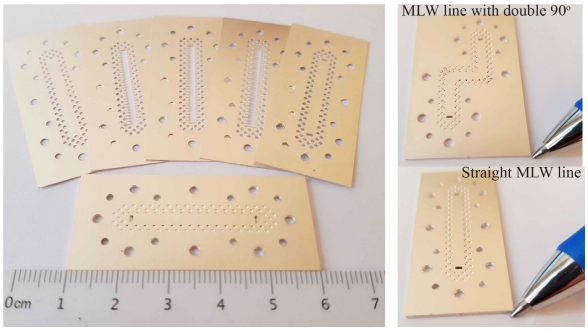

FIGURE 14. Photograph of the D-band multi-layer rectangular waveguide realized employing GW concept fabricated employing chemical metallic etching [147].

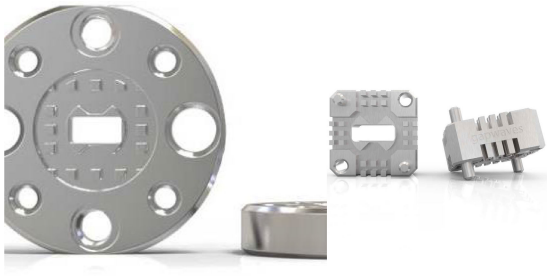

FIGURE 15. Gap waveguide flange commercialized by Gapwaves AB, Sweden.

the metallic layer being coated afterward [99], [100], [114], [140], [146]. Although 3D-printing has provided substantial manufacturing flexibility and sufficient accuracy for the fabrication of GW-based components operated at mmWave band, the surface roughness of the 3D-printed remains the most critical issue [142], [146]. This high surface roughness causes a produced GW antenna to become exceedingly lossy [142]. Furthermore, the use of 3D printing for manufacturing for the manufacture of GW-components is still in the research stage; its practicability for large-scale production is still unclear and requires additional research.

Recently, chemical metallic etching has been proposed as a method for producing GW-based filters [147], [148]. Fig. 14 illustrates the GW-based filter fabricated using chemical metallic etching. This chemical metallic etching is similar to the traditional PCB manufacturing. However, only metallic layers are present. In addition, it is a mature manufacturing technology that allows the production of GW-based devices at a large scale at a low cost. The metallic layer thickness selection is crucial for this manufacturing method, which typically requires very thin metallic layers. As a result, the AMC structure can be achieved with a relatively thin metallic sheet. Due to this requirement of the thin metallic layer, this manufacturing technique could only work to fabricate the prototype above 70 GHz with acceptable fabrication tolerances [148]. On the other hand, this manufacturing approach is best suited for the sub-THz band ($\geq$ 100 GHz), and the AMC structure could be easily realized using thin metallic plates [147].

VII. GW-TECHNOLOGY TOWARD THE INDUSTRIAL APPLICATIONS

With the technology evolving and promising demonstrations in several applications, GW technology has gained significant industrial interest. One substantial proof is the expansion of Gapwaves AB, Sweden, a spin-off company based on GW technology founded by the GW inventor, Per-Simon Kildal. In general, the patent of the GW transmission line concept is held by Gapwaves AB [149]. Thus most of the commercialized products are mainly coming from them. This section examines some of the product innovations based on GW-technology principles that have been disclosed by Gapwaves AB, Sweden, as well as other companies.

As discussed in previous sections, the GW-technology enables the creation of a wide range of devices. Other waveguide technologies, including standard metallic and substrate-integrated waveguides, may theoretically be used to create similar devices. One of the industry's major problems is the large-scale testing of waveguide components. Typically, waveguide-based technology testing requires connecting the devices' input to the output of the waveguide flange. A proper electrical connection is essential in waveguide-based (either conventional waveguide or SIW) devices to guarantee the products are tested reliably and to avoid unwanted passive intermodulation; this generally necessitates a considerable labor expense only to ensure the connector is securely connected to the input of the waveguide devices. One frequent strategy utilized in the SIW is to have a lossy transition from the SIW to the CPW line, verified with a standard connector. Gapwaves AB has developed a better and more reliable solution for dealing with the production test of waveguide devices known as GW-flange adapters, as shown in Fig. 15. This flange adapter may be mounted over the connection output linked to the vector network analyzer (VNA), and the input of the WG-based goods to be tested can be positioned directly on top of it. This is because GW technology promises to eliminate the requirement for electrical contact for waveguide input/output adapters, allowing items to be tested fast and reliably without the need for screws. Moreover, as indicated earlier, this GW-flange could eliminate the unwanted passive intermodulation caused by the non-perfect electrical connection. This resulted in substantial labor cost savings and time savings for large-scale production testing. To this end, the flange adapter operating at different frequencies ranging from K- to W-band are commercialized by Gapwave AB. Gapwaves AB has also filed multiple patents for GW-based phased array antennas and low-loss filters [150], [151]. These phased array antennas are primarily intended for usage in mmWave 5G and automobile radar applications as illustrated in Fig. 16.

Besides Gapwaves AB, other companies such as Telefonaktiebolaget LM Ericsson (SE), and Nidec Corporation (JP) have shown a significant interest in the GW-technology.

TABLE 7. Comparison of different fabrication technology for fully metallic gap waveguide components at large-scale industrial production. CNC is computer numerical control milling, and EDM is die-sink electric discharge machining.

Manufacturing Technology		CNC	EDM	3D Printing	Chemical Metallic Etching
Production Time		★★	★★★★	★	★★★★★
Technology Accessbility		★★★★★	★★	★★★★★	★★★★★
Fabrication Accuracy	at mmWave	★★★★★	★★★★	★★★★	★★★
	at sub-THz	★★★★	N/A	★	★★★
Cost	at mmWave	★★★	★★★★	★★★★★	★★★★★
	at sub-THz	★★	N/A	★★	★★★★★

Scale: ★ = very unfavourable; ★★ =unfavourable; ★★★ = average; ★★★★ = favorable; ★★★★★ = very favourable.

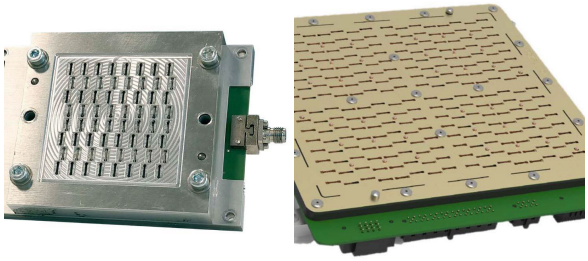

FIGURE 16. Millimeter-wave gap-waveguide phased array antenna for 5G communication commercialized by Gapwaves AB, Sweden [61], [63].

Numerous patents have been submitted by Telefonaktiebolaget LM Ericsson (SE), as an extension of the GW-technology idea. For example, they have suggested the glide symmetry meta-cell as a substitute for the AMC pin often utilized in GW as an alternate technique in designing AMC structures [152]. This idea was further expanded with the filing of a patent for the design of a flange connection to eliminate leakage in a waveguide [153] and the design of a leaky-wave antenna [154] based on the glide-symmetric principle. Nidec Corporation (JP), on the other hand, has integrated numerous electromagnetic wave transmission technologies, such as open waveguide, with GW-technology to construct multiple 3D array antenna and phased array slot antenna [155], [156], [157]. Metasum AB (SE) recently also filed a patent for a new type of transmission line, the so-called Multilayer Waveguide (MLW), based on the notion of GW-technology, to make GW-technology substantially simpler to manufacture [158]. Moreover, Huawei Technologies (CN) is also looking into how the GW technology can be combined with the conventional waveguide to improve the microwave devices' performance [159]. Samsung Electronics (KR) has also filed a patent on a different approach to implementing the ridge GW by realizing the AMC pin utilizing the substrate-integrated mushroom structure in conjunction with an all-metallic ridge [160].

On the other hand, another intriguing aspect of GW technology is its unique packaging potential for electronic devices. This has also drawn significant attention from the industry. Several industries have investigated the possibility of employing GW technology for packaging electronics circuits developed with other conventional transmission lines. For example, Telefonaktiebolaget LM Ericsson (SE) has filed a patent based on the transitions from multiple traditional transmission line technologies to GW technology and vice versa [161]. Furthermore, Veoneer US, Inc has filed many patents employing GW-technology for the packaging of the automotive radar sensor [162], [163], [164]. Moreover, Huber and Suhner AG (CH) has also filed a patent on designing an adaptor structure based on GW technology to have a good transition from the PCB circuit to the antenna structures [165].

Most of the above patents are related to wireless communication and the automotive industries. Aside from the patents discussed in this section, several collaborative publishing initiatives involving academia and industry were discussed in our previous session and will not be discussed further here.

VIII. CONCLUSION AND REMARKS

The state-of-the-art in gap waveguide (GW) technology is given in this article. First, the fundamental notion of GW technology is presented. Moreover, various GW-based antennas, such as slot array antennas, microstrip antennas, phased array antennas, leaky-wave antennas, and horn antennas, are summarised with highlights on the choices of GW types and their performance evaluations. This article also reviews and compares several GW-based passive circuits, such as beamforming networks, filters, and diplexers. Furthermore, packaging and high-density integration are essential parts of the establishment and implementation of mass-producible, cost-effective, and high-performance commercial products. Furthermore, the employment of GW technology for packaging may aid in resolving electromagnetic compatibility (EMC) concerns, particularly radiation emission and immunity problems. Additionally, reliable and cost-effective production technology is critical for bringing GW technology to market. This article discusses numerous frequently used manufacturing technologies to fabricate GW devices. Finally, we review and update current industrial interests and developments in GW technology by reviewing patents submitted by the industry.

Based on an assessment of current mmWave and sub-THz research related to the development of GW technology, the following future results are predicted.

1) **GW-based phased array transceiver with grating lobes-free 2D-scanning capabilities.** The phased array antenna is the key technology holder for Non-Line-of-Sight (NLoS) communications. Although

various phased array antennas have been constructed employing GW technology, most of these designs have remained 1D-scanning compatible. In [61], the 2D-beam scanning GW-phased array antenna is presented for the 5G mmWave band. However, the suggested phased array antenna is incompatible with applications that demand a wide scanning field of view over the H-plane. As a result, additional research is needed to develop the GW-based phased array antenna with 2D scanning.

2) **Evaluation of the functionality of the GW-based devices in harsh environments.** In general, fully metallic GW, such as GGW and RGW, offer superior compatibility in harsh environments. To this purpose, however, most of these GW-based devices remained evaluated and verified in a familiar environment. Although some work has been done to analyze the devices packed employing GW technology to function in the harsh electromagnetic environment, additional research is needed to investigate the operation of GW-based devices in other environmental variables, such as cryogenic conditions. This is critical for broadening the applicability of GW technology, particularly for space-based communication systems.
3) **Gap-waveguide-based tunable or reconfigurable devices.** Recently, a reconfigurable GW-based phased shifters were presented [59], [97], [98]. The reconfigurability is achieved by mechanical tuning [59], [97] or by embedding the GW with liquid crystal [98]. These studies provide a new avenue to investigate the invention of more complicated GW-based devices such as frequency reconfigurable filters or reconfigurable array antennas. Furthermore, additional research should be conducted to construct GW-based devices with other novel materials, such as graphene materials, that can enable reconfigurability capabilities.
4) **Design of a novel artificial magnetic conductor (AMC) for GW.** Traditionally, the AMC structure used for the GW is either 3D pins forming a bed of nails or a bed of nails. Although GW technology has overcome the manufacturing challenges of traditional hollow waveguides, manufacturing these 3D AMC pins remains complicated and may be quite expensive. Even though the glide-symmetric holey structures have decreased manufacturing complexity, the size of the AMC structures has increased by at least 2.5 times owing to the need for at least two rows of holes structures [23]. This enormous hole size has limited various uses, particularly antenna design. Given the suggested multi-metallic-layer air-filled waveguide in [147], a novel innovation of the AMC structure with a compact size and fabricable through the chemical metallic etching method is required for large-scale and cost-effective production. With the recent evolution of microwave photonics, new research opportunities have emerged to investigate the possibility of integrating GW-based devices with photonic circuits or packaging photonic circuits with GW.
5) **Evaluation of the manufacturing accuracy for different fabrication technologies of Gap Waveguide.** Numerous fabrication technology for the realization of the GW components have been presented. However, there is a need to study and compare the accuracy and their fabrication boundary, especially at higher frequencies such as the THz band.

ACKNOWLEDGMENT

The authors would like to thank Gapwaves AB for providing pictures of their products based on gapwaveguide technology. The author Andrés Alayón Glazunov was with the University of Twente at the time of submission of this work.

REFERENCES

[1] S. Rangan, T. S. Rappaport, and E. Erkip, "Millimeter-wave cellular wireless networks: Potentials and challenges," *Proc. IEEE*, vol. 102, no. 3, pp. 366–385, Mar. 2014.
[2] T. S. Rappaport, Y. Xing, O. Kanhere, S. Ju, A. Madanayake, S. Mandal, A. Alkhateeb, and G. C. Trichopoulos, "Wireless communications and applications above 100 GHz: Opportunities and challenges for 6G and beyond," *IEEE Access*, vol. 7, pp. 78729–78757, 2019.
[3] K. Wu, M. Bozzi, and N. J. G. Fonseca, "Substrate integrated transmission lines: Review and applications," *IEEE J. Microw.*, vol. 1, no. 1, pp. 345–363, Jan. 2021.
[4] T. Baras and A. F. Jacob, "Manufacturing reliability of LTCC millimeter-wave passive components," *IEEE Trans. Microw. Theory Techn.*, vol. 56, no. 11, pp. 2574–2581, Nov. 2008.
[5] K. Wu, Y. J. Cheng, T. Djerafi, and W. Hong, "Substrate-integrated millimeter-wave and terahertz antenna technology," *Proc. IEEE*, vol. 100, no. 7, pp. 2219–2232, Jul. 2012.
[6] M. Zhang, J. Hirokawa, and M. Ando, "An E-band partially corporate feed uniform slot array with laminated quasi double-layer waveguide and virtual PMC terminations," *IEEE Trans. Antennas Propag.*, vol. 59, no. 5, pp. 1521–1527, May 2011.
[7] M. Bozzi, A. Georgiadis, and K. Wu, "Review of substrate-integrated waveguide circuits and antennas," *IET Microw., Antennas Propag.*, vol. 5, no. 8, pp. 909–920, Jun. 2011.
[8] F. Zhu, G. Q. Luo, B. You, X. H. Zhang, and K. Wu, "Planar dual-mode bandpass filters using perturbed substrate-integrated waveguide rectangular cavities," *IEEE Trans. Microw. Theory Techn.*, vol. 69, no. 6, pp. 3048–3057, Jun. 2021.
[9] B. Chen, S. K. Thapa, A. Barakat, and R. K. Pokharel, "A W-band compact substrate integrated waveguide bandpass filter with defected ground structure in CMOS technology," *IEEE Trans. Circuits Syst. II, Exp. Briefs*, vol. 69, no. 3, pp. 889–893, Mar. 2022.
[10] P.-S. Kildal, E. Alfonso, A. Valero-Nogueira, and E. Rajo-Iglesias, "Local metamaterial-based waveguides in gaps between parallel metal plates," *IEEE Antennas Wireless Propag. Lett.*, vol. 8, pp. 84–87, 2009.
[11] P.-S. Kildal, "Artificially soft and hard surfaces in electromagnetics," *IEEE Trans. Antennas Propag.*, vol. 38, no. 10, pp. 1537–1544, Oct. 1990.
[12] E. Rajo-Iglesias, M. Ferrando-Rocher, and A. U. Zaman, "Gap waveguide technology for millimeter-wave antenna systems," *IEEE Commun. Mag.*, vol. 56, no. 7, pp. 14–20, Jul. 2018.
[13] S. Rahiminejad, E. Pucci, V. Vassilev, P. Kildal, S. Haasl, and P. Enoksson, "Polymer gap adapter for contactless, robust, and fast measurements at 220–325 GHz," *J. Microelectromech. Syst.*, vol. 25, no. 1, pp. 160–169, Feb. 2016.
[14] M. Ebrahimpouri, A. A. Brazalez, L. Manholm, and O. Quevedo-Teruel, "Using glide-symmetric holes to reduce leakage between waveguide flanges," *IEEE Microw. Wireless Compon. Lett.*, vol. 28, no. 6, pp. 473–475, Jun. 2018.
[15] X. Chen, D. Sun, W. Cui, and Y. He, "A folded contactless waveguide flange for low passive-intermodulation applications," *IEEE Microw. Wireless Compon. Lett.*, vol. 28, no. 10, pp. 864–866, Oct. 2018.

[16] D. Sievenpiper, L. Zhang, R. F. J. Broas, N. G. Alexopolous, and E. Yablonovitch, "High-impedance electromagnetic surfaces with a forbidden frequency band," *IEEE Trans. Microw. Theory Techn.*, vol. 47, no. 11, pp. 2059–2074, Nov. 1999.

[17] E. Rajo-Iglesias and P.-S. Kildal, "Numerical studies of bandwidth of parallel-plate cut-off realised by a bed of nails, corrugations and mushroom-type electromagnetic bandgap for use in gap waveguides," *IET Microw., Antennas Propag.*, vol. 5, no. 3, pp. 282–289, Feb. 2011.

[18] S. I. Shams and A. A. Kishk, "Double cone ultra wide band unit cell in ridge gap waveguides," in *Proc. IEEE Antennas Propag. Soc. Int. Symp. (APSURSI)*, Jul. 2014, pp. 1768–1769.

[19] E. Rajo-Iglesias, P. Kildal, A. U. Zaman, and A. Kishk, "Bed of springs for packaging of microstrip circuits in the microwave frequency range," *IEEE Trans. Compon., Packag., Manuf. Technol.*, vol. 2, no. 10, pp. 1623–1628, Oct. 2012.

[20] F. Fan, J. Yang, V. Vassilev, and A. U. Zaman, "Bandwidth investigation on half-height pin in ridge gap waveguide," *IEEE Trans. Microw. Theory Techn.*, vol. 66, no. 1, pp. 100–108, Jan. 2018.

[21] J. Yang, F. Fan, P. Taghikhani, and A. Vosoogh, "Half-height-pin gap waveguide technology and its applications in high gain planar array antennas at millimeter wave frequency," *IEICE Trans. Commun.*, vol. E101.B, no. 2, pp. 285–292, 2018.

[22] M. Ebrahimpouri, O. Quevedo-Teruel, and E. Rajo-Iglesias, "Design guidelines for gap waveguide technology based on glide-symmetric holey structures," *IEEE Microw. Wireless Compon. Lett.*, vol. 27, no. 6, pp. 542–544, Jun. 2017.

[23] M. Ebrahimpouri, E. Rajo-Iglesias, Z. Sipus, and O. Quevedo-Teruel, "Cost-effective gap waveguide technology based on glide-symmetric holey EBG structures," *IEEE Trans. Microw. Theory Techn.*, vol. 66, no. 2, pp. 927–934, Feb. 2018.

[24] A. U. Zaman and P. Kildal, "Wide-band slot antenna arrays with single-layer corporate-feed network in ridge gap waveguide technology," *IEEE Trans. Antennas Propag.*, vol. 62, no. 6, pp. 2992–3001, Jun. 2014.

[25] A. Vosoogh and P. Kildal, "Corporate-fed planar 60-GHz slot array made of three unconnected metal layers using AMC pin surface for the gap waveguide," *IEEE Antennas Wireless Propag. Lett.*, vol. 15, pp. 1935–1938, 2016.

[26] A. Vosoogh, A. Haddadi, A. U. Zaman, J. Yang, H. Zirath, and A. A. Kishk, "W-band low-profile monopulse slot array antenna based on gap waveguide corporate-feed network," *IEEE Trans. Antennas Propag.*, vol. 66, no. 12, pp. 6997–7009, Dec. 2018.

[27] X. Ding, J. An, X. Bu, H. Han, J. Liu, and Z. S. He, "A 16 × 16-element slot array fed by double-layered gap waveguide distribution network at 160 GHz," *IEEE Access*, vol. 8, pp. 55372–55382, 2020.

[28] S. A. Razavi, P.-S. Kildal, L. Xiang, E. A. Alós, and H. Chen, "2 × 2-slot element for 60-GHz planar array antenna realized on two doubled-sided PCBs using SIW cavity and EBG-type soft surface fed by microstrip-ridge gap waveguide," *IEEE Trans. Antennas Propag.*, vol. 62, no. 9, pp. 4564–4573, Sep. 2014.

[29] B. Cao, H. Wang, Y. Huang, and J. Zheng, "High-gain L-probe excited substrate integrated cavity antenna array with LTCC-based gap waveguide feeding network for W-band application," *IEEE Trans. Antennas Propag.*, vol. 63, no. 12, pp. 5465–5474, Dec. 2015.

[30] A. Vosoogh, P. Kildal, and V. Vassilev, "Wideband and high-gain corporate-fed gap waveguide slot array antenna with ETSI class II radiation pattern in *V*-band," *IEEE Trans. Antennas Propag.*, vol. 65, no. 4, pp. 1823–1831, Apr. 2017.

[31] A. Farahbakhsh, D. Zarifi, and A. U. Zaman, "60-GHz groove gap waveguide based wideband *H*-plane power dividers and transitions: For use in high-gain slot array antenna," *IEEE Trans. Microw. Theory Techn.*, vol. 65, no. 11, pp. 4111–4121, Nov. 2017.

[32] X. Jiang, F. Jia, Y. Cao, P. Huang, J. Yu, X. Wang, and Y. Shi, "Ka-band 8 × 8 low-sidelobe slot antenna array using a 1-to-64 high-efficiency network designed by new printed RGW technology," *IEEE Antennas Wireless Propag. Lett.*, vol. 18, no. 6, pp. 1248–1252, Jun. 2019.

[33] J. Liu, A. Vosoogh, A. U. Zaman, and J. Yang, "Design and fabrication of a high-gain 60-GHz cavity-backed slot antenna array fed by inverted microstrip gap waveguide," *IEEE Trans. Antennas Propag.*, vol. 65, no. 4, pp. 2117–2122, Apr. 2017.

[34] M. Ferrando-Rocher, A. Valero-Nogueira, J. I. Herranz-Herruzo, and J. Teniente, "60 GHz single-layer slot-array antenna fed by groove gap waveguide," *IEEE Antennas Wireless Propag. Lett.*, vol. 18, no. 5, pp. 846–850, May 2019.

[35] A. Farahbakhsh, D. Zarifi, and A. U. Zaman, "A mmWave wideband slot array antenna based on ridge gap waveguide with 30% bandwidth," *IEEE Trans. Antennas Propag.*, vol. 66, no. 2, pp. 1008–1013, Feb. 2018.

[36] W. Y. Yong, A. Haddadi, T. Emanuelsson, and A. A. Glazunov, "A bandwidth-enhanced cavity-backed slot array antenna for mmWave fixed-beam applications," *IEEE Antennas Wireless Propag. Lett.*, vol. 19, no. 11, pp. 1924–1928, Nov. 2020.

[37] T. Zhang, R. Tang, L. Chen, S. Yang, X. Liu, and J. Yang, "Ultra-wideband full-metal planar array antenna with a combination of ridge gap waveguide and E-plane groove gap waveguide," *IEEE Trans. Antennas Propag.*, vol. 70, no. 9, pp. 8051–8058, Sep. 2022.

[38] M. Ferrando-Rocher, J. I. Herranz-Herruzo, A. Valero-Nogueira, and B. Bernardo-Clemente, "Full-metal K-Ka dual-band shared-aperture array antenna fed by combined ridge-groove gap waveguide," *IEEE Antennas Wireless Propag. Lett.*, vol. 18, no. 7, pp. 1463–1467, Jul. 2019.

[39] M. Ferrando-Rocher, J. I. Herranz-Herruzo, A. Valero-Nogueira, and M. Baquero-Escudero, "Dual-band single-layer slot array antenna fed by K/Ka-band dual-mode resonators in gap waveguide technology," *IEEE Antennas Wireless Propag. Lett.*, vol. 20, no. 3, pp. 416–420, Mar. 2021.

[40] M. Akbari, A. Farahbakhsh, and A. Sebak, "Ridge gap waveguide multi-level sequential feeding network for high-gain circularly polarized array antenna," *IEEE Trans. Antennas Propag.*, vol. 67, no. 1, pp. 251–259, Jan. 2019.

[41] M. Ferrando-Rocher, J. I. Herranz-Herruzo, A. Valero-Nogueira, and A. Vila-Jiménez, "Single-layer circularly-polarized *Ka*-band antenna using gap waveguide technology," *IEEE Trans. Antennas Propag.*, vol. 66, no. 8, pp. 3837–3845, Aug. 2018.

[42] M. Ferrando-Rocher, J. I. Herranz-Herruzo, A. Valero-Nogueira, and B. Bernardo-Clemente, "Dual circularly polarized aperture array antenna in gap waveguide for high-efficiency Ka-band satellite communications," *IEEE Open J. Antennas Propag.*, vol. 1, pp. 283–289, 2020.

[43] Z. Zang, A. U. Zaman, and J. Yang, "Single layer dual circularly polarized antenna array based on ridge gap waveguide for 77 GHz automotive radar," *IEEE Trans. Antennas Propag.*, vol. 70, no. 7, pp. 5977–5982, Jul. 2022.

[44] M. Ferrando-Rocher, J. I. Herranz-Herruzo, A. Valero-Nogueira, B. Bernardo-Clemente, A. U. Zaman, and J. Yang, "8 × 8 *Ka*-band dual-polarized array antenna based on gap waveguide technology," *IEEE Trans. Antennas Propag.*, vol. 67, no. 7, pp. 4579–4588, Jul. 2019.

[45] J. Ran, C. Jin, P. Zhang, W. Wang, and Y. Wu, "High-gain and low-loss dual-polarized antenna array with reduced sidelobe level based on gap waveguide at 28 GHz," *IEEE Antennas Wireless Propag. Lett.*, vol. 21, no. 5, pp. 1022–1026, May 2022.

[46] D. Zarifi, A. Farahbakhsh, and A. U. Zaman, "A gap waveguide-fed wideband patch antenna array for 60-GHz applications," *IEEE Trans. Antennas Propag.*, vol. 65, no. 9, pp. 4875–4879, Sep. 2017.

[47] P. Sadri-Moshkenani, J. Rashed-Mohassel, and M. Shahabadi, "Microstrip antenna array fed by a low-loss gap-waveguide feed network," *IEEE Trans. Antennas Propag.*, vol. 66, no. 8, pp. 4359–4363, Aug. 2018.

[48] M. S. Sorkherizi, A. Dadgarpour, and A. A. Kishk, "Planar high-efficiency antenna array using new printed ridge gap waveguide technology," *IEEE Trans. Antennas Propag.*, vol. 65, no. 7, pp. 3772–3776, Jul. 2017.

[49] M. M. M. Ali, I. Afifi, and A. Sebak, "A dual-polarized magneto-electric dipole antenna based on printed ridge gap waveguide technology," *IEEE Trans. Antennas Propag.*, vol. 68, no. 11, pp. 7589–7594, Nov. 2020.

[50] E. Baghernia, R. Movahedinia, and A. Sebak, "Broadband compact circularly polarized spiral antenna array fed by printed gap waveguide for millimeter-wave applications," *IEEE Access*, vol. 9, pp. 86–95, 2021.

[51] E. Baghernia, M. M. M. Ali, and A. R. Sebak, "2 × 2 slot spiral cavity-backed antenna array fed by printed gap waveguide," *IEEE Access*, vol. 8, pp. 170609–170617, 2020.

[52] T. Li and Z. N. Chen, "Wideband sidelobe-level reduced *Ka*-band metasurface antenna array fed by substrate-integrated gap waveguide using characteristic mode analysis," *IEEE Trans. Antennas Propag.*, vol. 68, no. 3, pp. 1356–1365, Mar. 2020.

[53] T. Zhang, L. Chen, S. M. Moghaddam, A. U. Zaman, and J. Yang, "Ultra-wideband linearly polarised planar bowtie array antenna with feeding network using dielectric-based inverted microstrip gap waveguide," *IET Microw., Antennas Propag.*, vol. 14, no. 6, pp. 485–490, May 2020.

[54] T. Zhang, L. Chen, S. M. Moghaddam, A. U. Zaman, and J. Yang, "Millimeter-wave ultrawideband circularly polarized planar array antenna using bold-C spiral elements with concept of tightly coupled array," *IEEE Trans. Antennas Propag.*, vol. 69, no. 4, pp. 2013–2022, Apr. 2021.

[55] T. Zhang, L. Chen, A. U. Zaman, and J. Yang, "Ultra-wideband millimeter-wave planar array antenna with an upside-down structure of printed ridge gap waveguide for stable performance and high antenna efficiency," *IEEE Antennas Wireless Propag. Lett.*, vol. 20, no. 9, pp. 1721–1725, Sep. 2021.

[56] A. T. Hassan and A. A. Kishk, "Efficient procedure to design large finite array and its feeding network with examples of ME-dipole array and microstrip ridge gap waveguide feed," *IEEE Trans. Antennas Propag.*, vol. 68, no. 6, pp. 4560–4570, Jun. 2020.

[57] J. Cao, H. Wang, S. Mou, S. Quan, and Z. Ye, "W-band high-gain circularly polarized aperture-coupled magneto-electric dipole antenna array with gap waveguide feed network," *IEEE Antennas Wireless Propag. Lett.*, vol. 16, pp. 2155–2158, 2017.

[58] H. Kirino and K. Ogawa, "A 76 GHz multi-layered phased array antenna using a non-metal contact metamaterial waveguide," *IEEE Trans. Antennas Propag.*, vol. 60, no. 2, pp. 840–853, Feb. 2012.

[59] D. Sánchez-Escuderos, J. I. Herranz-Herruzo, M. Ferrando-Rocher, and A. Valero-Nogueira, "True-time-delay mechanical phase shifter in gap waveguide technology for slotted waveguide arrays in Ka-band," *IEEE Trans. Antennas Propag.*, vol. 69, no. 5, pp. 2727–2740, May 2021.

[60] Y. Zhang, A. R. Vilenskiy, and M. V. Ivashina, "Wideband open-ended ridge gap waveguide antenna elements for 1-D and 2-D wide-angle scanning phased arrays at 100 GHz," *IEEE Antennas Wireless Propag. Lett.*, vol. 21, no. 5, pp. 883–887, May 2022.

[61] C. Bencivenni, T. Emanuelsson, and M. Gustafsson, "Gapwaves platform integrates 5G mmWave arrays," *5G Phased Array Technol.*, vol. 20, no. 10, p. 23, 2019.

[62] A. Bagheri, C. Bencivenni, M. Gustafsson, and A. A. Glazunov, "A 28 GHz 8 × 8 gapwaveguide phased array employing GaN front-end with 60 dBm EIRP," *IEEE Trans. Antennas Propag.*, vol. 71, no. 5, pp. 4510–4515, May 2023.

[63] A. Bagheri, H. Karlsson, C. Bencivenni, M. Gustafsson, T. Emanuelsson, M. Hasselblad, and A. A. Glazunov, "A 16 × 16 45° slant-polarized gapwaveguide phased array with 65-dBm EIRP at 28 GHz," *IEEE Trans. Antennas Propag.*, vol. 71, no. 2, pp. 1319–1329, Feb. 2023.

[64] M. M. M. Ali and A. Sebak, "2-D scanning magnetoelectric dipole antenna array fed by RGW Butler matrix," *IEEE Trans. Antennas Propag.*, vol. 66, no. 11, pp. 6313–6321, Nov. 2018.

[65] I. Afifi and A. Sebak, "Wideband 4 × 4 Butler matrix in the printed ridge gap waveguide technology for millimeter-wave applications," *IEEE Trans. Antennas Propag.*, vol. 68, no. 11, pp. 7670–7675, Nov. 2020.

[66] C. Ma, S. Y. Zheng, Y. M. Pan, and Z. Chen, "Millimeter-wave fully integrated dielectric resonator antenna and its multi-beam application," *IEEE Trans. Antennas Propag.*, vol. 70, no. 8, pp. 6571–6580, Aug. 2022.

[67] Y. Quan, H. Wang, S. Tao, and J. Yang, "A wideband endfire double dipole antenna fed from double-ridge gap waveguides for multibeam array application," *IEEE Antennas Wireless Propag. Lett.*, vol. 21, no. 4, pp. 760–764, Apr. 2022.

[68] C. Wang, Y. Yao, X. Cheng, Z. Zhu, and X. Li, "A W-band high-efficiency multibeam circularly polarized antenna array fed by GGW Butler matrix," *IEEE Antennas Wireless Propag. Lett.*, vol. 20, no. 7, pp. 1130–1134, Jul. 2021.

[69] K. Wu, Y. Yao, X. Cheng, J. Yu, and X. Chen, "Design of millimeter-wave circularly polarized endfire antenna and multibeam antenna array for wireless applications," *IEEE Trans. Antennas Propag.*, vol. 69, no. 12, pp. 8397–8406, Dec. 2021.

[70] Y. Quan, H. Wang, S. Tao, and J. Yang, "A double-layer multibeam antenna with 45° linear polarization based on gap waveguide technology," *IEEE Trans. Antennas Propag.*, vol. 70, no. 1, pp. 56–66, Jan. 2022.

[71] N. Ashraf, A. Sebak, and A. A. Kishk, "PMC packaged single-substrate 4 × 4 Butler matrix and double-ridge gap waveguide horn antenna array for multibeam applications," *IEEE Trans. Microw. Theory Techn.*, vol. 69, no. 1, pp. 248–261, Jan. 2021.

[72] O. Zetterstrom, M. Petek, P. Castillo-Tapia, Á. Palomares-Caballero, N. J. G. Fonseca, and O. Quevedo-Teruel, "V-band fully metallic geodesic Luneburg lens antenna," *IEEE Trans. Antennas Propag.*, vol. 71, no. 2, pp. 1965–1970, Feb. 2023.

[73] P. Castillo-Tapia, O. Zetterstrom, A. Algaba-Brazález, L. Manholm, M. Johansson, N. J. G. Fonseca, and O. Quevedo-Teruel, "Two-dimensional beam steering using a stacked modulated geodesic Luneburg lens array antenna for 5G and beyond," *IEEE Trans. Antennas Propag.*, vol. 71, no. 1, pp. 487–496, Jan. 2023.

[74] D. R. Jackson, C. Caloz, and T. Itoh, "Leaky-wave antennas," *Proc. IEEE*, vol. 100, no. 7, pp. 2194–2206, Jul. 2012.

[75] M. Al Sharkawy and A. A. Kishk, "Long slots array antenna based on ridge gap waveguide technology," *IEEE Trans. Antennas Propag.*, vol. 62, no. 10, pp. 5399–5403, Oct. 2014.

[76] M. Al Sharkawy, A. Foroozesh, A. A. Kishk, and R. Paknys, "A robust horn ridge gap waveguide launcher for metal strip grating leaky wave antenna," *IEEE Trans. Antennas Propag.*, vol. 62, no. 12, pp. 6019–6026, Dec. 2014.

[77] M. R. Rahimi, N. Bayat-Makou, and A. A. Kishk, "Millimeter-wave substrate integrated gap waveguide leaky-wave antenna for WiGig applications," *IEEE Trans. Antennas Propag.*, vol. 67, no. 9, pp. 5790–5800, Sep. 2019.

[78] M. Vukomanovic, J. Vazquez-Roy, O. Quevedo-Teruel, E. Rajo-Iglesias, and Z. Sipus, "Gap waveguide leaky-wave antenna," *IEEE Trans. Antennas Propag.*, vol. 64, no. 5, pp. 2055–2060, May 2016.

[79] N. Memeletzoglou and E. Rajo-Iglesias, "Holey metasurface prism for the reduction of the dispersion of gap waveguide leaky-wave antennas," *IEEE Antennas Wireless Propag. Lett.*, vol. 18, no. 12, pp. 2582–2586, Dec. 2019.

[80] Q. Chen, O. Zetterstrom, E. Pucci, A. Palomares-Caballero, P. Padilla, and O. Quevedo-Teruel, "Glide-symmetric holey leaky-wave antenna with low dispersion for 60 GHz point-to-point communications," *IEEE Trans. Antennas Propag.*, vol. 68, no. 3, pp. 1925–1936, Mar. 2020.

[81] S. Wang, Z. Li, B. Wei, S. Liu, and J. Wang, "A Ka-band circularly polarized fixed-frequency beam-scanning leaky-wave antenna based on groove gap waveguide with consistent high gains," *IEEE Trans. Antennas Propag.*, vol. 69, no. 4, pp. 1959–1969, Apr. 2021.

[82] E. Pucci, E. Rajo-Iglesias, J. Vázquez-Roy, and P. Kildal, "Planar dual-mode horn array with corporate-feed network in inverted microstrip gap waveguide," *IEEE Trans. Antennas Propag.*, vol. 62, no. 7, pp. 3534–3542, Jul. 2014.

[83] N. Bayat-Makou and A. A. Kishk, "Millimeter-wave substrate integrated dual level gap waveguide horn antenna," *IEEE Trans. Antennas Propag.*, vol. 65, no. 12, pp. 6847–6855, Dec. 2017.

[84] M. Hamedani, H. Oraizi, A. Amini, D. Zarifi, and A. U. Zaman, "Planar H-plane horn antenna based on groove gap waveguide technology," *IEEE Antennas Wireless Propag. Lett.*, vol. 19, no. 2, pp. 302–306, Feb. 2020.

[85] D. Cao, Y. Li, J. Wang, F. Sun, and L. Ge, "Millimeter-wave three-dimensional substrate-integrated OMT-fed horn antenna using vertical and planar groove gap waveguides," *IEEE Trans. Microw. Theory Techn.*, vol. 69, no. 10, pp. 4448–4459, Oct. 2021.

[86] M. Mohammadpour, F. Mohajeri, and S. A. Razavi, "A new wide band and compact H-plane horn antenna based on groove gap waveguide technology," *IEEE Trans. Antennas Propag.*, vol. 70, no. 1, pp. 221–228, Jan. 2022.

[87] Y. Quan, J. Yang, H. Wang, and A. U. Zaman, "An unequal power divider based on ridge gap waveguide with an inserted conductor plate," *Microw. Opt. Technol. Lett.*, vol. 63, no. 2, pp. 443–449, Feb. 2021.

[88] J. Liu, F. Yang, K. Fan, and C. Jin, "Unequal power divider based on inverted microstrip gap waveguide and its application for low sidelobe slot array antenna at 39 GHz," *IEEE Trans. Antennas Propag.*, vol. 69, no. 12, pp. 8415–8425, Dec. 2021.

[89] A. K. Nobandegani and S. E. Hosseini, "Gysel power divider realized by ridge gap waveguide technology," *IEEE Access*, vol. 9, pp. 72103–72110, 2021.

[90] A. Karimi Nobandegani and S. E. Hosseini, "Bagley polygon power divider realized by ridge gap waveguide technology," *Microw. Opt. Technol. Lett.*, vol. 63, no. 5, pp. 1406–1410, May 2021.

[91] H. Huang, Y. Wu, W. Wang, W. Feng, and Y. Shi, "Analysis of the propagation constant of a ridge gap waveguide and its application of dual-band unequal couplers," *IEEE Trans. Plasma Sci.*, vol. 48, no. 12, pp. 4163–4170, Dec. 2020.

[92] M. M. M. Ali, M. S. El-Gendy, M. Al-Hasan, I. B. Mabrouk, A. Sebak, and T. A. Denidni, "A systematic design of a compact wideband hybrid directional coupler based on printed RGW technology," *IEEE Access*, vol. 9, pp. 56765–56772, 2021.

[93] Z. Zhao and T. A. Denidni, "Millimeter-wave printed-RGW hybrid coupler with symmetrical square feed," *IEEE Microw. Wireless Compon. Lett.*, vol. 30, no. 2, pp. 156–159, Feb. 2020.

[94] E. Rajo-Iglesias, M. Ebrahimpouri, and O. Quevedo-Teruel, "Wideband phase shifter in groove gap waveguide technology implemented with glide-symmetric holey EBG," *IEEE Microw. Wireless Compon. Lett.*, vol. 28, no. 6, pp. 476–478, Jun. 2018.

[95] A. Palomares-Caballero, A. Alex-Amor, P. Padilla, F. Luna, and J. Valenzuela-Valdes, "Compact and low-loss V-band waveguide phase shifter based on glide-symmetric pin configuration," *IEEE Access*, vol. 7, pp. 31297–31304, 2019.

[96] Á. Palomares-Caballero, C. Megías, C. Molero, A. Alex-Amor, and P. Padilla, "Wideband gap-waveguide phase shifter based on a glide-symmetric ridge," *IEEE Microw. Wireless Technol. Lett.*, vol. 33, no. 1, pp. 27–30, Jan. 2023.

[97] Á. Palomares-Caballero, A. Alex-Amor, P. Escobedo, J. Valenzuela-Valdés, and P. Padilla, "Low-loss reconfigurable phase shifter in gap-waveguide technology for mm-wave applications," *IEEE Trans. Circuits Syst. II, Exp. Briefs*, vol. 67, no. 12, pp. 3058–3062, Dec. 2020.

[98] M. Nickel, A. Jiménez-Sáez, P. Agrawal, A. Gadallah, A. Malignaggi, C. Schuster, R. Reese, H. Tesmer, E. Polat, D. Wang, P. Schumacher, R. Jakoby, D. Kissinger, and H. Maune, "Ridge gap waveguide based liquid crystal phase shifter," *IEEE Access*, vol. 8, pp. 77833–77842, 2020.

[99] A. Tamayo-Domínguez, J. Fernández-González, and M. Sierra-Castañer, "3-D-printed modified Butler matrix based on gap waveguide at W-band for monopulse radar," *IEEE Trans. Microw. Theory Techn.*, vol. 68, no. 3, pp. 926–938, Mar. 2020.

[100] A. Tamayo-Domínguez, J. Fernández-González, and M. Sierra-Castañer, "Monopulse radial line slot array antenna fed by a 3-D-printed cavity-ended modified Butler matrix based on gap waveguide at 94 GHz," *IEEE Trans. Antennas Propag.*, vol. 69, no. 8, pp. 4558–4568, Aug. 2021.

[101] L. F. Carrera-Suárez, D. V. Navarro-Méndez, M. Baquero-Escudero, and A. Valero-Nogueira, "Rotman lens with ridge-gap waveguides, implemented in LTCC technology, for 60 GHz applications," in *Proc. 9th Eur. Conf. Antennas Propag. (EuCAP)*, Apr. 2015, pp. 1–5.

[102] J. Pourahmadazar, M. Farahani, and T. Denidni, "Printed ridge gap waveguide Rotman lens for millimetre-wave applications," in *Proc. 18th Int. Symp. Antenna Technol. Appl. Electromagn. (ANTEM)*, Aug. 2018, pp. 1–2.

[103] D. Pérez-Quintana, C. Bilitos, J. Ruiz-García, I. Ederra, J. Teniente-Vallinas, D. González-Ovejero, and M. Beruete, "Fully metallic Luneburg metalens antenna in gap waveguide technology at V-band," *IEEE Trans. Antennas Propag.*, vol. 71, no. 4, pp. 2930–2937, Apr. 2023.

[104] A. A. Brazalez, A. U. Zaman, and P. Kildal, "Improved microstrip filters using PMC packaging by lid of nails," *IEEE Trans. Compon., Packag., Manuf. Technol.*, vol. 2, no. 7, pp. 1075–1084, Jul. 2012.

[105] A. Vosoogh, A. A. Brazález, and P. Kildal, "A V-band inverted microstrip gap waveguide end-coupled bandpass filter," *IEEE Microw. Wireless Compon. Lett.*, vol. 26, no. 4, pp. 261–263, Apr. 2016.

[106] A. K. Horestani and M. Shahabadi, "Balanced filter with wideband common-mode suppression in groove gap waveguide technology," *IEEE Microw. Wireless Compon. Lett.*, vol. 28, no. 2, pp. 132–134, Feb. 2018.

[107] M. S. Sorkherizi and A. A. Kishk, "Self-packaged, low-loss, planar bandpass filters for millimeter-wave application based on printed gap waveguide technology," *IEEE Trans. Compon., Packag., Manuf. Technol.*, vol. 7, no. 9, pp. 1419–1431, Sep. 2017.

[108] S. Birgermajer, N. Janković, V. Radonić, V. Crnojević-Bengin, and M. Bozzi, "Microstrip-ridge gap waveguide filter based on cavity resonators with mushroom inclusions," *IEEE Trans. Microw. Theory Techn.*, vol. 66, no. 1, pp. 136–146, Jan. 2018.

[109] H. Golboni, M. Arezoomand, A. Pirhadi, and S. Asadi, "Design of high-selective printed-ridge gap waveguide filter using source–load and cross couplings," *IEEE Microw. Wireless Compon. Lett.*, vol. 30, no. 6, pp. 557–560, Jun. 2020.

[110] J. Chen, D. Shen, X. Zhang, and Y. Sa, "Integrated substrate groove gap waveguide and application for filter design," *Int. J. RF Microw. Comput.-Aided Eng.*, vol. 31, no. 11, p. e22830, Nov. 2021.

[111] M. Sharifi Sorkherizi and A. A. Kishk, "Completely tuned coupled cavity filters in defected bed of nails cavity," *IEEE Trans. Compon., Packag., Manuf. Technol.*, vol. 6, no. 12, pp. 1865–1872, Dec. 2016.

[112] M. Mazinani, M. Arezoomand, and A. Pirhadi, "Ku-band gap waveguide filter design with improved out of band response," *Microw. Opt. Technol. Lett.*, vol. 60, no. 9, pp. 2154–2161, Sep. 2018.

[113] D. Sun and J. Xu, "A novel iris waveguide bandpass filter using air gapped waveguide technology," *IEEE Microw. Wireless Compon. Lett.*, vol. 26, no. 7, pp. 475–477, Jul. 2016.

[114] B. Al-Juboori, J. Zhou, Y. Huang, M. Hussein, A. Alieldin, W. J. Otter, D. Klugmann, and S. Lucyszyn, "Lightweight and low-loss 3-D printed millimeter-wave bandpass filter based on gap-waveguide," *IEEE Access*, vol. 7, pp. 2624–2632, 2019.

[115] J. L. Vazquez-Roy, E. Rajo-Iglesias, G. Ulisse, and V. Krozer, "Design and realization of a band pass filter at D-band using gap waveguide technology," *J. Infr., Millim., THz Waves*, vol. 41, no. 12, pp. 1469–1477, Dec. 2020.

[116] J. Deng, D. Yuan, J. Yin, D. Sun, L. Guo, X. Ma, and Y. Hao, "Ultracompact bandpass filter based on slow wave substrate integrated groove gap waveguide," *IEEE Trans. Microw. Theory Techn.*, vol. 70, no. 2, pp. 1211–1220, Feb. 2022.

[117] Z. Liu, J. Deng, and D. Sun, "Slow-wave groove gap waveguide bandpass filter," *IEEE Access*, vol. 7, pp. 52581–52588, 2019.

[118] M. Baquero-Escudero, A. Valero-Nogueira, M. Ferrando-Rocher, B. Bernardo-Clemente, and V. E. Boria-Esbert, "Compact combline filter embedded in a bed of nails," *IEEE Trans. Microw. Theory Techn.*, vol. 67, no. 4, pp. 1461–1471, Apr. 2019.

[119] B. Ahmadi and A. Banai, "Direct coupled resonator filters realized by gap waveguide technology," *IEEE Trans. Microw. Theory Techn.*, vol. 63, no. 10, pp. 3445–3452, Oct. 2015.

[120] T. Xiu, Y. Yao, H. Jiang, X. Cheng, C. Wang, B. Wang, J. Yu, and X. Chen, "Design of a compact and low-loss E-band filter based on multilayer groove gap waveguide," *IEEE Microw. Wireless Compon. Lett.*, vol. 31, no. 11, pp. 1211–1214, Nov. 2021.

[121] W. Y. Yong, A. Hadaddi, and A. A. Glazunov, "Design and characterization of the fully metallic gap waveguide-based frequency selective radome for millimeter wave fixed beam array antenna," *IEEE Trans. Antennas Propag.*, vol. 71, no. 1, pp. 531–541, Jan. 2023.

[122] H. S. Farahani, R. A. Sadeghzadeh, N. Gharanfeli, and A. A. Kishk, "Novel design of microwave diplexers using gap waveguide technology," *Microw. Opt. Technol. Lett.*, vol. 59, no. 5, pp. 1133–1136, May 2017.

[123] D. Zarifi, A. Shater, A. Ashrafian, and M. Nasri, "Design of Ku-band diplexer based on groove gap waveguide technology," *Int. J. RF Microw. Comput.-Aided Eng.*, vol. 28, no. 9, p. e21487, Nov. 2018.

[124] A. Vosoogh, M. S. Sorkherizi, A. U. Zaman, J. Yang, and A. A. Kishk, "An integrated Ka-band diplexer-antenna array module based on gap waveguide technology with simple mechanical assembly and no electrical contact requirements," *IEEE Trans. Microw. Theory Techn.*, vol. 66, no. 2, pp. 962–972, Feb. 2018.

[125] M. Rezaee and A. U. Zaman, "Realisation of carved and iris groove gap waveguide filter and E-plane diplexer for V-band radio link application," *IET Microw., Antennas Propag.*, vol. 11, no. 15, pp. 2109–2115, Dec. 2017.

[126] C. Sanchez-Cabello, L. F. Herran, and E. Rajo-Iglesias, "Ka-band diplexer for 5G mmWave applications in inverted microstrip gap waveguide technology," *Electronics*, vol. 9, no. 12, p. 2094, Dec. 2020.

[127] X. He and T. H. Hubing, "A closed-form expression for estimating the maximum radiated emissions from a heatsink on a printed circuit board," *IEEE Trans. Electromagn. Compat.*, vol. 54, no. 1, pp. 205–211, Feb. 2012.

[128] E. Rajo-Iglesias, A. U. Zaman, and P.-S. Kildal, "Parallel plate cavity mode suppression in microstrip circuit packages using a lid of nails," *IEEE Microw. Wireless Compon. Lett.*, vol. 20, no. 1, pp. 31–33, Jan. 2010.

[129] Y. Shi, M. Zhou, and J. Zhang, "Parallel plate mode suppression in low-frequency microwave circuit packages using lid of 3-D cross by a 3-D printing technique," *IEEE Trans. Electromagn. Compat.*, vol. 59, no. 4, pp. 1268–1271, Aug. 2017.

[130] X. Yang, L. Zhang, Y. Li, H. Jin, P. Cheng, Y. Li, and E. Li, "A novel package lid using mushroom-type EBG structures for unintentional radiation mitigation," *IEEE Trans. Electromagn. Compat.*, vol. 60, no. 6, pp. 1882–1888, Dec. 2018.

[131] A. U. Zaman, M. Alexanderson, T. Vukusic, and P. Kildal, "Gap waveguide PMC packaging for improved isolation of circuit components in high-frequency microwave modules," *IEEE Trans. Compon., Packag., Manuf. Technol.*, vol. 4, no. 1, pp. 16–25, Jan. 2014.

[132] A. Uz Zaman, T. Vukusic, M. Alexanderson, and P. Kildal, "Design of a simple transition from microstrip to ridge gap waveguide suited for MMIC and antenna integration," *IEEE Antennas Wireless Propag. Lett.*, vol. 12, pp. 1558–1561, 2013.

[133] U. Nandi, A. U. Zaman, A. Vosoogh, and J. Yang, "Novel millimeter wave transition from microstrip line to groove gap waveguide for MMIC packaging and antenna integration," *IEEE Microw. Wireless Compon. Lett.*, vol. 27, no. 8, pp. 691–693, Aug. 2017.

[134] J. M. Pérez-Escudero, A. E. Torres-García, R. Gonzalo, and I. Ederra, "A Chebyshev transformer-based microstri-to-groove-gap-waveguide inline transition for MMIC packaging," *IEEE Trans. Compon., Packag., Manuf. Technol.*, vol. 9, no. 8, pp. 1595–1602, Aug. 2019.

[135] A. Hassona, V. Vassilev, A. U. Zaman, V. Belitsky, and H. Zirath, "Compact low-loss chip-to-waveguide and chip-to-chip packaging concept using EBG structures," *IEEE Microw. Wireless Compon. Lett.*, vol. 31, no. 1, pp. 9–12, Jan. 2021.

[136] J. Zhang, X. Zhang, D. Shen, and A. A. Kishk, "Packaged microstrip line: A new quasi-TEM line for microwave and millimeter-wave applications," *IEEE Trans. Microw. Theory Techn.*, vol. 65, no. 3, pp. 707–719, Mar. 2017.

[137] B. Ahmadi and A. Banai, "Substrateless amplifier module realized by ridge gap waveguide technology for millimeter-wave applications," *IEEE Trans. Microw. Theory Techn.*, vol. 64, no. 11, pp. 3623–3630, Nov. 2016.

[138] W. Yu, A. Vosoogh, B. Wang, and Z. S. He, "Substrateless packaging for a D-band MMIC based on a waveguide with a glide-symmetric EBG hole configuration," *Sensors*, vol. 22, no. 17, p. 6696, Sep. 2022.

[139] A. Vosoogh, M. S. Sorkherizi, V. Vassilev, A. U. Zaman, Z. S. He, J. Yang, A. A. Kishk, and H. Zirath, "Compact integrated full-duplex gap waveguide-based radio front end for multi-Gbit/s point-to-point backhaul links at E-band," *IEEE Trans. Microw. Theory Techn.*, vol. 67, no. 9, pp. 3783–3797, Sep. 2019.

[140] M. Ferrando-Rocher, J. I. Herranz-Herruzo, A. Valero-Nogueira, and B. Bernardo-Clemente, "Performance assessment of gap-waveguide array antennas: CNC milling versus three-dimensional printing," *IEEE Antennas Wireless Propag. Lett.*, vol. 17, no. 11, pp. 2056–2060, Nov. 2018.

[141] A. Vosoogh, A. U. Zaman, V. Vassilev, and J. Yang, "Zero-gap waveguide: A parallel plate waveguide with flexible mechanical assembly for mm-wave antenna applications," *IEEE Trans. Compon., Packag., Manuf. Technol.*, vol. 8, no. 12, pp. 2052–2059, Dec. 2018. [Online]. Available: https://ieeexplore.ieee.org/document/8514044/

[142] A. Vosoogh, "Compact RF integration and packaging solutions based on metasurfaces for millimeter-wave applications," Ph.D. thesis, Dept. Elect. Eng., Antenna Group, Chalmers Univ. Technol., Gothenburg, Sweden, 2018.

[143] J. E. A. Qudeiri, A. Zaiout, A.-H.-I. Mourad, M. H. Abidi, and A. Elkaseer, "Principles and characteristics of different EDM processes in machining tool and die steels," *Appl. Sci.*, vol. 10, no. 6, p. 2082, Mar. 2020.

[144] W. J. Otter and S. Lucyszyn, "Hybrid 3-D-printing technology for tunable THz applications," *Proc. IEEE*, vol. 105, no. 4, pp. 756–767, Apr. 2017.

[145] H. Xin and M. Liang, "3-D-printed microwave and THz devices using polymer jetting techniques," *Proc. IEEE*, vol. 105, no. 4, pp. 737–755, Apr. 2017.

[146] Y. Cheng and Y. Dong, "Wideband dual-polarized gap waveguide antenna array based on novel 3-D-printed feeding-network topologies," *IEEE Trans. Antennas Propag.*, vol. 71, no. 2, pp. 1493–1505, Feb. 2023.

[147] A. Vosoogh, H. Zirath, and Z. S. He, "Novel air-filled waveguide transmission line based on multilayer thin metal plates," *IEEE Trans. THz Sci. Technol.*, vol. 9, no. 3, pp. 282–290, May 2019.

[148] A. Vosoogh, A. A. Brazález, Y. Li, and Z. S. He, "A compact mass-producible E-band bandpass filter based on multi-layer waveguide technology," in *Proc. 14th Eur. Conf. Antennas Propag. (EuCAP)*, Mar. 2020, pp. 1–5.

[149] P.-S. Kildal, "Waveguides and transmission lines in gaps between parallel conducting surfaces," U.S. Patent 8 803 638, Aug. 12, 2014.

[150] C. Bencivenni, "High frequency filter and phased array antenna comprising such a high frequency filter," U.S. Patent 17/271 235, Sep. 30, 2021.

[151] T. Emanuelsson, Y. Jian, A. U. Zaman, and W. Yong, "Antenna array based on one or more metamaterial structures," U.S. Patent 17/426 237, Apr. 7, 2022.

[152] O. Q. Teruel, M. Mattsson, A. A. Brazalez, L. Manholm, K. Andersson, and M. Johansson, "Parallel plate unit cell for a parallel plate arrangement," U.S. Patent 17/288 332, Dec. 9, 2021.

[153] A. A. Brazalez, L. Manholm, and O. Q. Teruel, "Waveguide interconnection with glide symmetrically positioned holes for avoiding leakage," U.S. Patent 16/647 891, Jul. 9, 2020.

[154] E. Pucci, O. Q. Teruel, and O. Dahlberg, "Leaky wave antenna," U.S. Patent 17/423 264, Mar. 10, 2022.

[155] H. Kirino and K. Hiroyuki, "Slot array antenna, and radar, radar system, and wireless communication system including the slot array antenna," U.S. Patent 16/016 913, Dec. 27, 2019.

[156] H. Kirino and K. Hiroyuki, "Slot array antenna, and radar, radar system, and wireless communication system including the slot array antenna," U.S. Patent 10 381 741, Aug. 13, 2019.

[157] K. Hiroyuki and H. Kirino, "Slot antenna devices," U.S. Patent 16/016 913, Dec. 27, 2019.

[158] A. Vosoogh and Z. S. He, "Multi-layer waveguide, arrangement, and method for production thereof," U.S. Patent 16/758 454, Aug. 6, 2020.

[159] O. Jian, "Planar waveguide, waveguide filter and antenna," CN Patent 14/144 026, Apr. 12, 2014.

[160] A. R. Vilenskiy, M. N. Makurin, and L. Chongmin, "Ridge gap waveguide and multilayer antenna array including the same," U.S. Patent 16/706 251, Jun. 11, 2020.

[161] R. Maaskant, A. Aljarosha, and A. U. Zaman, "Transition arrangement comprising a contactless transition or connection between an SIW and a waveguide or an antenna," U.S. Patent 10 381 317, Aug. 13, 2019.

[162] S. B. Doyle, R. J. Sletten, and A. Alexanian, "Waveguide sensor assemblies and related methods," U.S. Patent 11 201 414, Dec. 14, 2021.

[163] S. B. Doyle, A. Alexanian, and K. Konstantinidis, "Combined waveguide and antenna structures and related sensor assemblies," U.S. Patent 11 196 171, Dec. 7, 2021.

[164] S. B. Doyle, A. Alexanian, and K. Konstantinidis, "Transitional waveguide structures and related sensor assemblies," U.S. Patent 11 283 162, Mar. 22, 2022.

[165] U. Hügel, R. Glogowski, M. Thiel, and F. Merli, "Adapter structure with waveguide channels," U.S. Patent 10 658 761, May 19, 2020.

WAI YAN YONG (Member, IEEE) received the bachelor's degree (Hons.) in electronic engineering from Universiti Tun Hussein Onn Malaysia (UTHM), Parit Raja, Johor, Malaysia, in 2016, and the Master of Philosophy degree in electrical engineering from Universiti Teknologi Malaysia (UTM), in 2018.

In August 2018, he joined the Radio System Group, University of Twente, The Netherlands, as a Marie Currie Ph.D. Researcher and worked on the WAVECOMBE Project which is funded by the European Union through the Marie Currie Horizon 2020. During the Ph.D. time, he is a Visiting Researcher with Gapwaves AB, Gothenburg, Sweden. In January 2023, he joined Rohde & Schwarz GmBH & Company KG., Munich, Germany, as the RF System Engineer for 5G/6G. His research interests include millimeter-wave and THz antenna array designs, frequency-selective surfaces, phased array transceivers, and new materials for antenna and microwave devices. He is a member of the IEEE Antenna and Propagation Society and the IEEE Microwave Theory and Technology Society. He was a recipient of the UTHM Chancellor's Award during the 16th UTHM Convocation. He was a recipient of the Best Postgraduate Student Award for the master's degree during the 60th UTM Convocation. He received the Vice Chancellor's Award and the Dean's List Award on the 16th UTHM Convocation. He received the JPA Scholarship sponsored by the Public Service Department Malaysia for the bachelor's degree study. He has also served as a Reviewer for IEEE Antenna and Propagation Letters, IEEE Access, *International Journal of Electronics and Communications*, *Frequenz*, and *Journal of Optics*.

ABBAS VOSOOGH received the M.Sc. degree from the K. N. Toosi University of Technology, Tehran, Iran, in 2011, and the Ph.D. degree from the Chalmers University of Technology, Gothenburg, Sweden, in 2018.

He is currently the Director of technology and innovation with Gapwaves AB, Sweden. His current research interests include system integration and packaging for millimeter- and submillimeter-wave applications, metasurfaces, passive components, and planar array antenna design. He was a recipient of the Best Student Paper Award from the 2015 International Symposium on Antennas and Propagation, TAS, Australia, the CST University Publication Award in 2016, the Best Paper Award and the Best Student Paper Award from the 2016 International Symposium on Antennas and Propagation, Okinawa, Japan, the First Prize Student Award from the 2017 IEEE International Symposium on Antennas and Propagation and USNC-URSI Radio Science Meeting, San Diego, CA, USA, and the 2019 EurAAP Kildal Award for Best Ph.D. in Antenna and Propagation.

ALIREZA BAGHERI received the bachelor's and master's degrees in electrical engineering from the Amirkabir University of Technology (Tehran Polytechnic), Tehran, Iran, in 2013 and 2016, respectively. He is currently pursuing the Ph.D. degree with the University of Twente, Enschede, The Netherlands, as a Marie Skłodowska-Curie Actions (MSCA) Fellow.

Then, he joined the Electromagnetic and Antenna Laboratory, Amirkabir University of Technology, as a Researcher. He is an Industrial Ph.D. Researcher with Gapwaves AB, Gothenburg, Sweden. His research interests include phased array antennas and microwave/mmWave engineering.

COEN VAN DE VEN (Graduate Student Member, IEEE) received the bachelor's and master's degrees in electrical engineering from the Technical University Eindhoven, The Netherlands, in 2019 and 2021, respectively. He is currently pursuing the industrial Ph.D. degree with the Department of Radio System Engineering, University of Twente, Enschede, The Netherlands.

He is an Antenna Engineer with Gapwaves AB, Gothenburg, Sweden. He is the Marie Curie Researcher funded by the European Union through the Marie Currie Horizon 2020 Project. His research interest includes the physical realization of antenna concepts, going from theory to architecture that can be produced for use in industry.

ABOLFAZL HADADDI received the Ph.D. degree from the Amirkabir University of Technology, Tehran, Iran. His Ph.D. thesis is entitled "Reflector Antenna Surface Distortions: Determination and Compensation." In March 2015, he was with the Chalmers University of Technology, Sweden, as a Visiting Researcher, where he worked on the hat and the eleven array antennas. He had worked in several research and development roles for research institutes in Iran. In 2017, he joined Gapwaves AB, Sweden, as a Senior Antenna Design Engineer. He is currently the Director of antenna innovation with Gapwaves AB. He is the author or coauthor of over 20 conference papers and journal articles. His main research interests include automotive radars, mmWave antenna systems, satellite communications, and 5G systems.

ANDRÉS ALAYÓN GLAZUNOV (Senior Member, IEEE) was born in Havana, Cuba. He received the M.Sc. (Engineer-Researcher) degree in physical engineering from Peter the Great St. Petersburg Polytechnic University (Polytech), St. Petersburg, Russia, in 1994, the Ph.D. degree in electrical engineering from Lund University, Lund, Sweden, in 2009, and the Docent (Habilitation) degree in antenna systems from the Chalmers University of Technology, Gothenburg, Sweden, in 2017.

From 1996 to 2005, he held various research and specialist positions in the telecom industry, such as Ericsson Research, Telia Research, and TeliaSonera, Stockholm, Sweden. From 2001 to 2005, he was the Swedish Delegate to the European Cost Action 273. From 2009 to 2010, he held a Marie Curie Senior Research Fellowship with the Centre for Wireless Network Design, University of Bedfordshire, Luton, U.K. From 2010 to 2014, he held a postdoctoral position with the Electromagnetic Engineering Laboratory, KTH Royal Institute of Technology, Stockholm. From 2014 to 2018, he was an Assistant Professor with the Chalmers University of Technology. From 2018 to 2023, he was an Associate Professor with the Department of Electrical Engineering, University of Twente, Enschede, The Netherlands, where he led the antenna systems, propagation, and OTA research. From 2018 to 2020, he was the Dutch Delegate to the European Cost Action IRACON. He is currently a Senior Associate Professor with Linköping University, Norrköping Campus, Sweden, where he is leading research in the design and characterization of intelligent devices and environments for communications, radar, and positioning applications. He has been one of the pioneers in producing the first standardized OTA measurement techniques for 3GPP and devising novel OTA techniques, such as random-LOS and hybrid antenna characterization techniques. He has contributed to or initiated various European research projects, such as more recently, the is3DMIMO, the WAVECOMBE, the 5VC, and the Build-Wise projects under the auspices of the H2020 European Research and Innovation Program. He has also contributed to the international 3GPP and the ITU standardization bodies. He is the author of more than 150 scientific and technical publications. He is the coauthor and the Co-Editor of the textbook *LTE-Advanced and Next Generation Wireless Networks–Channel Modelling and Propagation* (Wiley, 2012). His current research interests include mmWave sensor array design, MIMO antenna systems, electromagnetic theory, fundamental limitations on antenna-channel interactions, radio propagation channel measurements, modeling and simulations, wireless performance in the built environment, and the OTA characterization of antenna systems and wireless devices.